Supporting Information for

Engineering NIR Rhodol Derivative with Spirocyclic Ring-opening Activation for High-Contrast Photoacoustic Imaging

Feng Liu, Xiao Shi, Xianjun Liu, Fenglin Wang*, Hai-Bo Yi, and Jian-Hui Jiang*

State Key Laboratory of Chemo/Bio-Sensing and Chemometrics, College of Chemistry and Chemical Engineering, Hunan University, Changsha, 410082, P. R. China

E-mail: jianhuijiang@hnu.edu.cn; fengliw@hnu.edu.cn

Table of Contents

Materials and Instruments

Dicoumarol and nicotinamide adenine dinucleotide (NADH) were purchased from Aladdin® (Los Angeles, USA). Human NAD(P)H: quinone oxidoreductase-1 (hNQO1), porcine liver esterase (PLE), monoamine oxidase-A (MAO-A), γ-glutamyl transferase (GGT), nitroreductase (NTR), cytochrome P450 reductase (CPR), glutathione-disulfide reductase (GSR) and methyl thiazolyltetrazolium (MTT) assay kit were purchased from Sigma-Aldrich (St. Louis, MO, USA). Hoechst 33342, Mito-Tracker® Green FM and Lyso-Tracker Green DND-26 were obtained from Invitrogen. H_2O_2, cysteine (Cys), glutathione (GSH) were obtained from J&K Chemicals (Beijing, China). HT-29 cells and MDA-MB-231 cells were supplied by the cell bank of Central Laboratory at Xiangya Hospital (Changsha, China). Female BALB/c nude mice (5 weeks old, weighing 19-22 g) were provided by Hunan Shrek Jingda Experimental Animal Cooperation (Changsha, China). All other reagents of analytical grade were purchased from Sinopharm Chemical Reagent (Shanghai, China), and used without further purification unless otherwise indicated. Ultrapure water with an electric resistance >18.2 MΩ was obtained from a Millipore Milli-Q water purification system (Billerica, MA).

Thin-layer chromatography (TLC) was performed on precoated silica gel 60 F254 (Qingdao Ocean Chemicals), and column chromatography was performed on silica gel (mesh 200-300, Qingdao Ocean Chemicals). Mass spectra (MS) were recorded on an LTQ Orbitrap Velos Pro mass spectrometer (Thermo Fisher Scientific, Bremen, Germany) and an LCQ Advantage ion trap mass spectrometry (Thermo Finnigan). ^{1}H NMR, ^{13}C NMR and ^{19}F NMR spectra were acquired on a Bruker DRX-400 NMR spectrometer (Bruker) using tetramethylsilane (TMS) as an internal standard. UV-vis absorption spectra were recorded on a UV-1800 spectrophotometer (Shimadzu, Japan). Fluorescence spectra were recorded with an FS5 spectrofluorometer (Edinburgh, UK) with excitation and emission slits of 5.0 nm. pH was determined using a Mettler-Toledo FE20 pH meter. HPLC analysis was performed with an Agilent 1260 Infinity liquid chromatograph (with a DAD). Fluorescence imaging of

cells was performed on a Nikon A1+ confocal microscope (Japan). All the photoacoustic imaging experiments were performed on a multispectral optoacoustic tomographic (MSOT) imaging system (inVision256-TF, iThera Medical GmbH). Fluorescence imaging of mice was performed on an IVIS Lumina XR small animal imaging system (Caliper, Switzerland).

Characterization of photophysical properties

All the tested compounds and probes including Rhodol-NIR1, Rhodol-NIR2, Rhodol-NIR, Rhodol-PA and the Control probe were dissolved in DMSO (10 mM) and stored at 4 ^{o}C for further use.

For determining the pKa values of Rhodol-NIR1, Rhodol-NIR2 and Rhodol-NIR, each compound was diluted with buffers of different pH values to final concentrations of 15 μM. Both absorbance and fluorescence spectra were acquired sequentially. For obtaining fluorescence spectra, 650 nm was used as the excitation wavelength for Rhodol-NIR1 and 620 nm was used for the remaining analogues. The pKa of the each compound was calculated according to the Henderson-Hasselbalch equation.

The quantum yield of Rhodol-NIR was determined in PBS (pH 7.4), using cresyl violet (Φ_S = 0.54 in MeOH) as a reference.[S1] The quantum yield was calculated according to Equation 1:

$$\Phi_X = \Phi_S (A_S F_X / A_X F_S) (n_X / n_S)^2 \qquad (1)$$

Φ: quantum yield; A: absorbance at the excitation wavelength; F: integral area of fluorescence spectra at the same excitation wavelength; n: the refractive index of solvents; S and X represent the reference standard and unknown sample, respectively.

For photostability studies, Rhodol-NIR (15 μM) was placed on a microscope and irradiated with a head mercury lamp (100 W). Fluorescence spectra were obtained at different time points. For comparison, indocyanine green (ICG) was also investigated under the same conditions. Maximum fluorescence intensities of Rhodol-NIR and ICG were plotted as a function of time.

TDDFT (Time-Dependent Density Functional Theory) Calculations

As was demonstrated by the UV-vis absorption and fluorescence spectra that Rhodol-NIR1 and Rhodol-NIR were predominately present in the spirocyclic ring-open form structure, we chose the phenoate forms, which are the resonance structures of the dissociated hydroxyl phenolic forms at pH 7.4 for theoretical calculations. The closed spirolactone structure of acetylated Rhodol-NIR was chosen for theoretical calculations. The ground state structures of Rhodol-NIR1, Rhodol-NIR2, Rhodol-NIR,

acetylated Rhodol-NIR, Control chromopohre and acetylated Control chromopohre were optimized with using DFT with CAM (Coulomb Attenuated Method)-B3LYP functional and 6-311++g** basis set.[S2] Initial geometries of all the compounds were generated with Hyperchem. UV-vis absorption was then performed with TDDFT using the optimized structure of the ground state (CAM-B3LYP/6-311++g**). All the calculations were performed with Gaussian 09 (Revision B. 01).

***In vitro* characterizations of Rhodol-PA**

For *in vitro* PA imaging, a microtube (200 μL) was filled with the sample and then placed into the tube holder for signal acquisition, using 680 nm as the excitation wavelength. For *in vitro* PA spectra, tubes filled with Rhodol-NIR or Rhodol-PA were scanned from 680 nm to 800 nm with an interval of 10 nm. Tubes filled with PBS was used as the control for background deduction. All MSOT data were acquired with the MSOT imaging system with the following parameters, excitation (680 nm-980 nm), pulse frequency (10 Hz), pulse length (8 ns) and maximal optical parametric oscillator energy (120 mJ at 740 nm). The light was delivered to the sample via a ring-type fiber bundle. The generated acoustic signals were collected with a 256-element transducer array.

Fluorescence spectra were recorded with an excitation wavelength of 620 nm. For *in vitro* response of Rhodol-PA towards hNQO1, 15 μM of Rhodol-PA was dissolved in PBS buffer (10 mM, pH = 7.4), containing 0.5% (v/v) DMSO and NADH (100 μM). To study the response of Rhodol-PA towards hNQO1, Rhodol-PA was incubated with hNQO1 (3.0 μg/mL) for 1.5 h, then photoacoustic, absorption and fluorescence signals were acquired, respectively. To test the ability of Rhodol-PA to quantify hNQO1, Rhodol-PA was incubated with different concentrations of hNQO1 (0-3.0 μg/mL), photoacoustic, absorption, and fluorescence signals were obtained, respectively. The photoacoustic signals at 680 nm, the absorption at 630 nm and fluorescence intensity at 720 nm were plotted against the concentrations of hNQO1, respectively. The detection limit was calculated according to Equation 2:

$$DL = 3\sigma/k \qquad (2)$$

DL: detection limit; σ: standard deviation of triplicate experiments; k: slopes of the linear fitting curves of absorbance, PA and fluorescence intensity toward the concentrations of hNQO1.

For selectivity assay, Rhodol-PA was incubated with various substances: (0) Blank; (1) Cys (1.0 mM); (2) GSH (1.0 mM); (3) H_2O_2 (0.5 mM); (4) Nicotinamide adenine dinucleotide (NADH) (0.5 mM); (5) γ-glutamyl transpeptadase (GGT) (100 U L^{-1}); (6) Porcine liver esterase (PLE) (10.0 μg/mL); (7) Monoamine oxidase-A (MAO-A) (10 μg/mL); (8) Nitroreductase (NTR) (2.0 μg/mL) + NADH (100 μM); (9) glutathione-disulfide reductase (GSR) (10.0 μg/mL) + NADH (100 μM); (10) cytochrome P450 reductase (CPR) (10.0 μg/mL) + NADH (100 μM) at 37 °C for 1.5 h. Afterwards, PA, absorption and fluorescence signals were acquired. For cell lysate experiment, Rhodol-PA was mixed with cell lysates of HT-29 (5 μL) or MDA-MB-231 (5 μL) at 37 °C for 1.5 h. PA, absorption and fluorescence signals were then obtained. For comparison, cell lysate of HT-29 (5 μL) was incubated with dicoumarol (100 μM) at 37 °C for 1 h. Rhodol-PA was added and the mixture was incubated at 37 °C for another 1.5 h before measurements.

The response time of Rhodol-PA toward hNQO1 was investigated via real-time fluorescence measurement. Rhodol-PA was incubated with hNQO1 (3.0 μg/mL), the fluorescence signals at 720 nm were recorded in real time. To study the effect of pH on the response of Rhodol-PA toward hNQO1, Rhodol-PA and hNQO1 (3.0 μg/mL) were mixed in buffers of different pH values. The solutions were incubated at 37 °C for 1.5 h before fluorescence measurement. The effect of pH on the stability of Rhodol-PA was studied under the same conditions.

Kinetic Assay

Different concentrations of Rhodol-PA (5, 10, 20, 30, 40, 60 μM) were incubated with hNQO1 (5.0 μg/mL^{-1}) at 37 °C for 1.5 h in PBS buffer (10 mM, pH = 7.4), containing 0.5% (v/v) DMSO and NADH (100 μM). Fluorescence spectra were recorded for quantification analysis. The initial reaction velocity (μM S^{-1}) was calculated, plotted against the concentrations of Rhodol-PA, and fitted to a Michaelis-

Menten curve. Kinetic parameters were calculated according to the Michaelis Menten equation: $V = V_{max}$ [probe] (K_m + [probe]), where V is the reaction rate, and [probe] is the concentration of Rhodol-PA (substrate).

HPLC and HRMS (ESI) analysis

HPLC chromatograms of Rhodol-PA, Rhodol-NIR and the reaction products of Rhodol-PA with hNQO1 were performed on a system with a C18 column (250 nm × 4.6 mm, 5 μm) with the following conditions: methanol/H_2O (0.2% CF_3COOH) = 90/10 (v/v); flow rate: 1 mL/min; detection wavelength: 550 nm. For further demonstration of the reaction mechanism, HRMS-ESI was introduced to analyze the products of Rhodol-PA with hNQO1. Rhodol-PA (15 μM) was incubated with hNQO1 (1.5 μg/mL) in PBS buffer (10 mM, pH = 7.4), containing 0.5% (v/v) DMSO and NADH (100 μM) for 1.5 h at 37 °C. The reaction mixture was then quenched with 1 mL MeCN, vortexed and centrifuged at 10000 rpm for 15 minutes. The supernatant was analyzed by mass spectrometry in positive mode.

Cell Culture and PA/Fluorescence Imaging

HT-29 cells were cultured in RPMI-1640 medium, supplemented with 10% fetal bovine serum, penicillin (100 U/mL) and streptomycin (100U/mL). MDA-MB-231 cells were grown in Dulbecco's modified Eagle's medium (DMEM) supplemented with 10% fetal bovine serum, penicillin (100 U/mL) and streptomycin (100 U/mL). Both cell lines were incubated at 37 °C in a humidified incubator containing 5% (v/v) CO_2.

PA images of cells were performed as follows: HT-29 or MDA-MB-231 cells (plated at high density, ~7×10^6 cells in a 75 cm^2 cell culture bottle) were incubated with Rhodol-PA (30 μM) at 37 °C for 2 h. The cells were washed with 10 mL PBS for three times. Cells were harvested with 0.25% trypsin and counted with a TC20™ automated cell counter (BIO-RAD, USA). The cell suspension was collected with a microtube (200 μL) by centrifugation. Tubes with the cell pellets were inserted into the tube holder and imaged with the MSOT imaging system. For inhibition study, HT-

29 cells were pretreated with dicoumarol (100 μM) for 1 h before incubation with Rhodol-PA (30 μM).

Confocal fluorescence images were performed according to the following procedure: HT-29 or MDA-MB-231 cells were incubated with 1 mL fresh culture medium containing Rhodol-PA (20 μM) at 37 °C for 1.5 h. The cells were washed with cold PBS for three times before imaging. For inhibition study, HT-29 cells were pretreated with dicoumarol (100 μM) for 1 h before incubation with Rhodol-PA (20 μM). Fluorescence images were acquired with a Nikon A1+ confocal microscope with an excitation wavelength of 640 nm and an emission region from 663 nm to 738 nm.

Subcellular colocalization assay

HT-29 cells cultured in 35-mm glass bottom culture dishes were incubated with Rhodol-PA (20 μM) for 1.5 h at 37 °C. Then, Hoechst 33342 (0.5 μg mL^{-1}), Mito-Tracker Green (0.5 μM), and Lyso-Tracker Green (100 nM) were added and incubated for another 30 min, respectively. The cells were washed with cold PBS twice before imaging. The following conditions were used for obtaining fluorescence images. The fluorescence signal for Rhodol-PA was collected from 663 nm to 738 nm with an excitation wavelength of 640 nm. To obtain fluorescence signals from LysoTracker Green DND 26 and MitoTracker Green FM, the emission wavelength was collected from 500 nm to 540 nm with an excitation wavelength of 488 nm. The fluorescence signal for Hoechst 33342 was collected from 440 nm to 480 nm with an excitation wavelength of 405 nm.

MTT assay

The cytotoxicity of Rhodol-PA against HT-29 and MDA-MB-231 cells were studied using a standard MTT assay. HT-29 and MDA-MB-231 cells were seeded into a 96-well plate at 5×10^3 cells/well in 100 μL culture medium, respectively. The cells were grown at 37 ^oC for 24 h. Then, cells were incubated with fresh culture medium containing various concentrations of Rhodol-PA (0-300 μM) for 12 h. Afterwards, the culture medium was removed and the cells were washed with cold

PBS for three times. The cells were incubated with MTT reagent (10 μL, 5 mg/mL) at 37 ^{o}C for 4 h. DMSO (100 μL/well) was then added for 10 min to dissolve the precipitated formazan violet crystals. The absorbance at 570 nm was recorded using an ELx800™ microplate reader.

Tumor Mouse Model

All animal experiments were approved by the Hunan Provincial Science & Technology Department and performed in compliance with the guidelines of the Institutional Animal Care and Use Committee of Human University. Female BALB/c nude mice (5 weeks old, 19-22 g) were used for establishing animal tumor models. A suspension of 5×10^6 HT-29 cells or MDA-MB-231 cells was subcutaneously implanted into the right oxter of each mouse. Tumor size was estimated as follows: $V = 0.5 \times \text{length} \times \text{width}^2$.

Intratumoral PA/NIRF Imaging

For intratumoral PA/NIRF imaging, tumors were grown to a size of 20-25 mm^3. The mouse was anesthetized by 1% isoflurane delivered via a nose cone during the experiments. Rhodol-PA (60 μM in 50 μL PBS) was intratumorally injected into the mice bearing HT-29 tumors or MDA-MB-231 tumors, respectively. Ultrasound gel was then applied to the mice before wrapping with polyethylene membrane to enable coupling between the tissue and water medium. The mouse was fixed with a double leg slide and placed in a water bath with a temperature of 34 °C for PA imaging at 680 nm through 800 nm with an interval of 10 nm and 850 nm (background). The entire tumor region was scanned with each wavelength with a step size of 0.3 mm. *In vivo* MSOT images were acquired before injection (0 min) and at a given time post injection. Guided ICA spectral unmixing was introduced to separate signals from the activated probes and those from the photoabsorbers in tissue (e.g. hemoglobin). The mean MSOT intensities were obtained with ViewMSOT from six different regions of interest (ROIs) from the tumor. The mean intensities at varied times post injection were all subjected to deduction of the background obtained before injection.

Fluorescence images of mice were captured on an IVIS Lumina XR small animal imaging system with an excitation filter of 605 nm and a Cy5.5 emission filter (690-750 nm). The anesthetized mice intratumorally injected with Rhodol-PA (60 μM in 50 μL PBS) were positioned into the imaging bin with the tumor in the field of view. Fluorescence images were acquired before injection (0 h) and at a given time post injection. All imaging parameters were kept the same for each acquisition. Data were analyzed with the Living Image 4.0 Software. ROIs of equal area in the tumor regions were obtained for further analysis.

***In vivo* PA/NIRF Imaging**

For PA/NIRF imaging upon tail vein injection, the tumors were grown to a size of 50-75 mm^3. For MSOT imaging, the mice were anesthetized with 1% isoflurane in oxygen. Rhodol-PA (300 μM in 200 μL sterilized PBS, equivalent to 2.56 mg kg^{-1}) was injected into mice bearing HT-29 tumors or MDA-MB-231 tumors via tail vein, respectively. For controls, sterilized PBS (200 μL) was injected instead. Ultrasound gel was then applied to the mice before wrapping with polyethylene membrane to enable coupling between the tissue and water medium. Each mouse was fixed with a double leg slide and placed in a water bath with a temperature of 34 °C for PA imaging at 680 nm through 800 nm with an interval of 10 nm and 850 nm (background). The entire tumor was scanned with each wavelength with a spacing of 0.3 mm. *In vivo* MSOT images were acquired before injection (0 min) and at a given time post injection. Guided ICA spectral unmixing was introduced to separate signals from the activated probes and those from photoabsorbers in tissues (e.g. hemoglobin). The mean MSOT intensities were obtained with ViewMSOT from six different ROIs from the tumor. The mean intensities at varied times post injection were all subjected to deduction of the background obtained before injection.

For NIRF imaging, Rhodol-PA (500 μM in 200 μL sterilized PBS, equivalent to 4.27 mg kg^{-1}) was injected into mice bearing HT-29 tumors or MDA-MB-231 tumors via tail vein, respectively. Fluorescence images of mice were captured on an IVIS Lumina XR small animal imaging system (Caliper, Switzerland) with an excitation

filter of 605 nm and a Cy5.5 emission filter (690-760 nm). The anesthetized mice were positioned into the imaging cabin with the tumors placed in the field of view. *In vivo* fluorescence images were acquired before injection (0 min) and at different time points post injection. All imaging parameters were kept constant throughout the experiments. Data were analyzed with the Living Image 4.0 Software. ROIs of equal area in the tumor regions were obtained for further analysis.

Biodistribution of Rhodol-PA

The biodistribution of Rhodol-PA in HT-29 tumor bearing mice was performed with an IVIS animal imaging system. Rhodol-PA (300 μM, 200 μL) was injected to different mice bearing HT-29 tumors, then mice were euthanized at different time points (5, 12 and 24 hours). Their major organs (heart, liver, spleen, lung, and kidney) and tumor were carefully harvested and rinsed with saline, placed onto petri dishes, and immediately imaged with the IVIS animal imaging system. HT-29 tumor bearing mice without injection of Rhodol-PA was used as a control. The fluorescence intensity of each organ and tumor was analyzed using the Living Image 4.0 Software.

Scheme S1. The structures of compounds

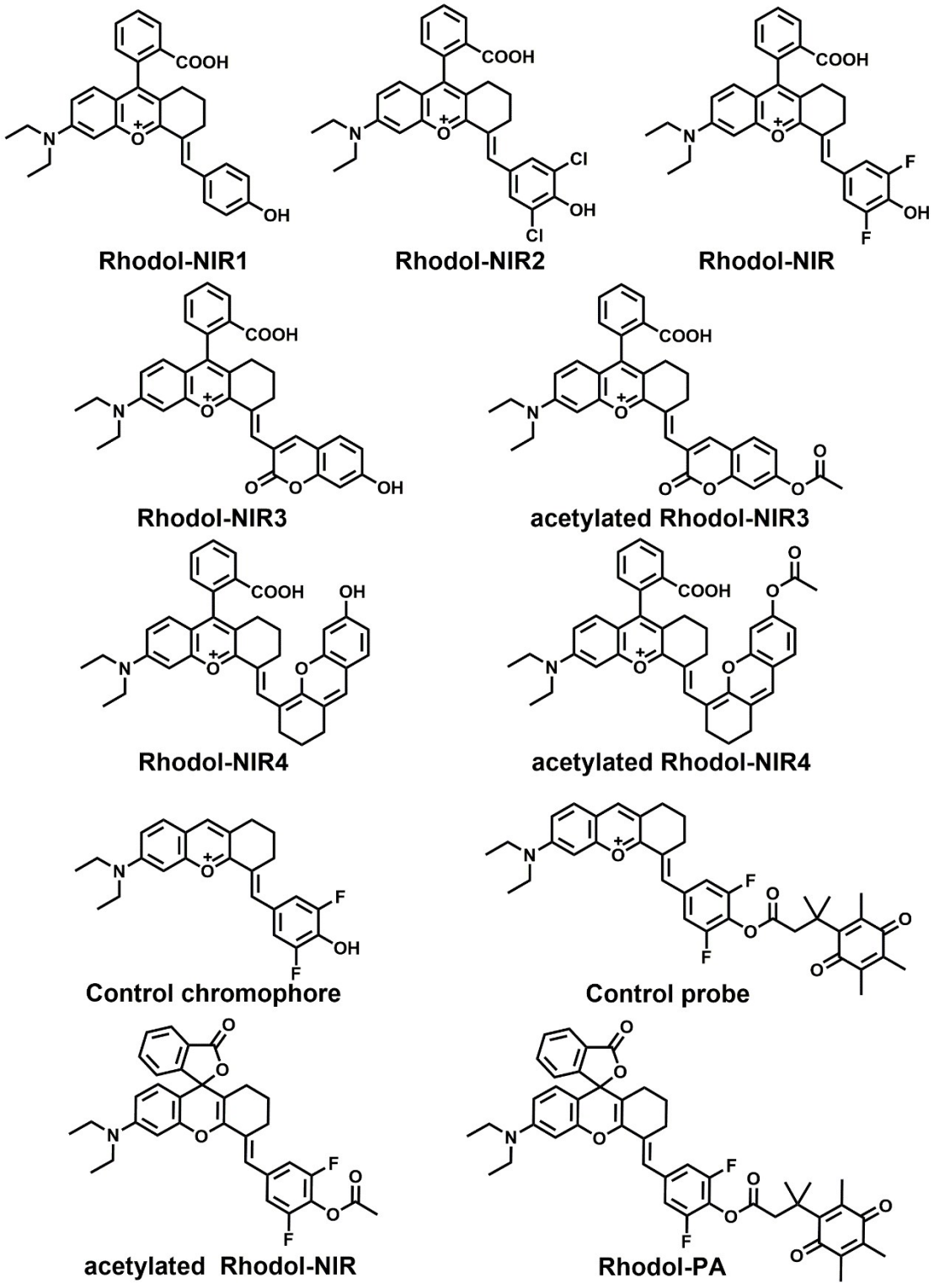

Synthetic procedures for intermediates and final compounds

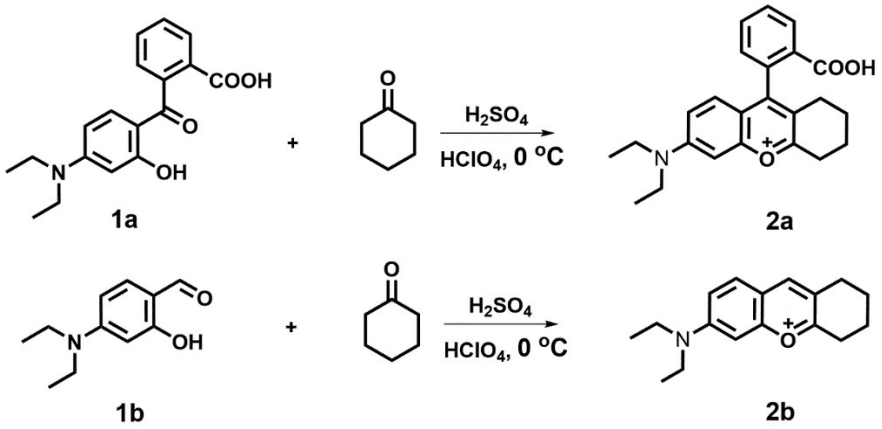

Compound 2a and 2b: Compound 2a and 2b were prepared according to literature with slight modifications.[S3] Particularly, freshly distilled cyclohexanone (3.3 mL, 31.9 mmol) was added dropwise to concentrated H_2SO_4 (35 mL) and the mixture was cooled down to 0 °C. Then, compound 1a or 1b (16 mmol) was added in portions while stirring. The mixture was poured to ice (150 g) after reaction at 90 °C for 1.5 h. Then, perchloric acid (70%; 3.5 mL) was added, and the resulting precipitate was filtered and washed with cold water (50 mL). Compound 2a and 2b were obtained as red solids and used without further purification.

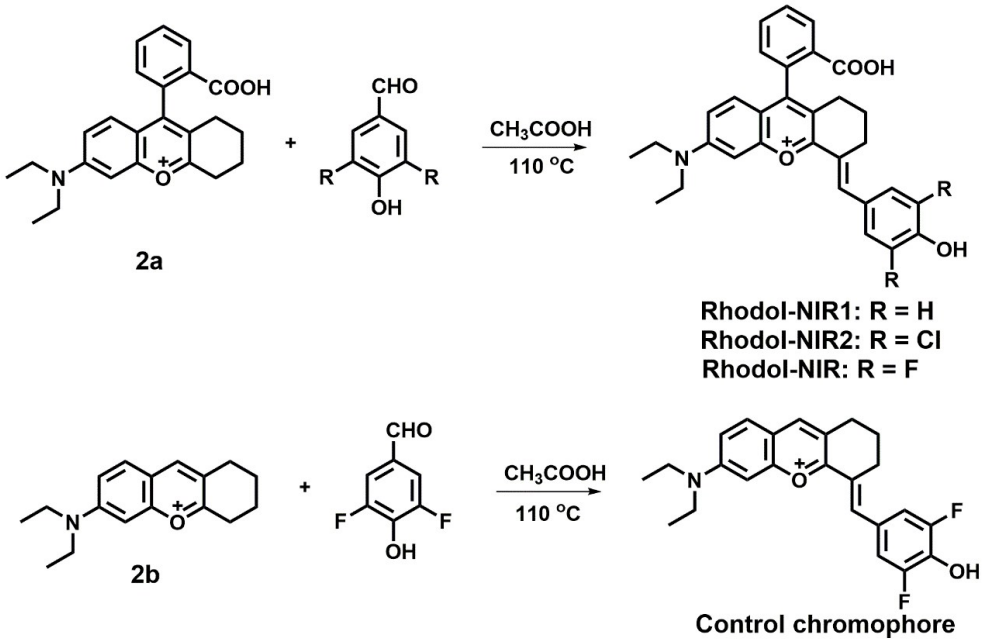

Rhodol-NIR1: Compound 2a (178.1 mg, 0.5 mmol) and 4-hydroxybenzaldehyde (91.5 mg, 0.75 mmol) were dissolved in acetic acid (10 mL), and the reaction mixture was heated to 110 °C overnight. The solvent was removed under reduced pressure to give the product, which was purified by silica gel flash chromatography (CH_2Cl_2/MeOH, 200/1 to 100/1) to obtain Rhodol-NIR1 as a blue solid (57.4 mg, yield 29%). ^{1}H NMR (400 MHz, CD_3OD): δ (ppm) 1.31-1.34 (t, J=4.0 Hz, 6H), 1.76-1.88 (m, 2H), 2.41-2.44 (t, J = 4.0 Hz, 2H), 2.94-2.96 (t, J = 4.0 Hz, 2H), 3.68-3.73 (m, 4H), 6.87-6.90 (d, 2H), 7.09-7.29 (m, 4H), 7.58-7.60 (m, 2H), 7.70-7.79 (m, 2H), 8.14 (s, 1H), 8.26-8.28 (d, J = 8.0 Hz, 1H). ^{13}C NMR (100 MHz, CD_3OD): δ (ppm) 11.46, 21.14, 25.62, 26.88, 45.47, 95.19, 115.45, 116.83, 117.00, 122.24, 125.59, 127.24, 127.62, 128.15, 129.54, 129.90, 130.64, 131.43, 133.18, 134.40, 137.45, 155.44, 158.50, 159.53, 162.54, 164.27. ESI-MS: m/z calcd for Rhodol-NIR1 ($C_{31}H_{30}NO_4^+$, $[M-ClO_4^-]^+$), 480.22; found, 480.33.

Rhodol-NIR2: Rhodol-NIR2, prepared similarly as Rhodol-NIR1 using Compound 2a (178.1 mg, 0.5 mmol) and 3,5-dichloro-4-hydroxybenzaldehyde (118.5 mg, 0.75 mmol), was obtained as a blue solid (57.4 mg, yield 29%). ^{1}H NMR (400 MHz, DMSO-d_6): δ (ppm) 8-1.11 (t, J = 8.0 Hz, 6H), 1.22 (s, 2H), 2.56-1.59 (m, 2H), 2.58-2.74 (m, 2H), 6.39-6.56 (m, 3H), 7.29-7.31(d, J = 8.0 Hz, 2H), 7.47 (s, 2H), 7.65-7.69

(t, J=8.0 Hz, 1H), 7.77-7.81(t, J=8.0 Hz, 3H), 7.94-7.96 (d, J=8.0 Hz, 1H). ^{13}C NMR (100 MHz, DMSO-d_6): δ (ppm) 12.86, 22.20, 23.16, 26.91, 29.47, 44.24, 97.19, 114.58, 109.76, 109.79, 108.84, 122.78, 124.33, 124.40,125.43,125.46, 125.49, 125.54, 127.32, 128.66, 130.02, 130.03, 130.35, 135.62, 149.74, 152.36, 169.32. ESI-MS: m/z calcd for Rhodol-NIR2 ($C_{31}H_{28}Cl_2NO_2^+$, [M-ClO_4^-]$^+$), 548.14; found, 548.20.

Rhodol-NIR: Rhodol-NIR, prepared similarly as Rhodol-NIR1 using compound 2a (237.6 mg, 0.5 mmol) and 3,5-difluoro-4-hydroxybenzaldehyde (118.5 mg, 0.75 mmol), was obtained Rhodol-NIR as a blue solid (89.2 mg, yield 29%). ^{1}H NMR (400 MHz, DMSO-d_6): δ (ppm) 1.20 (t, 6H), 1.67-1.73 (d, J = 24.0 Hz, 2H), 2.13 (s, 2H), 2.85 (m, 2H), 3.59 (s, 4H), 6.84 (s, 1H), 7.10 (s, 2H), 7.33-7.38 (t, J = 8.0 Hz, 3H), 7.75-7.85 (m, 3H), 8.14-8.15 (d, J = 4.0 Hz, 2H). ^{13}C NMR (100 MHz, DMSO-d_6): δ (ppm) 12.94, 21.62, 26.69, 29.46, 45.54, 96.24, 114.37, 114.43, 114.48, 114.51, 114.58, 129.13, 129.79, 129.81, 130.68, 134.17, 134.20, 134.24, 151.15, 151.23, 153.56, 153.63, 167.67. ^{19}F NMR (400 MHz, DMSO-d_6): δ (ppm) -131.88, -131.86. HRMS (ESI) m/z calcd for Rhodol-NIR ($C_{31}H_{28}F_2NO_2^+$, [M-ClO_4^-]$^+$), 516.1981; found, 516.1985.

Control chromopohre: The Control chromophore was prepared similarly as Rhodol-NIR1 using compound 2b (178.1 mg, 0.5 mmol) and 4-hydroxybenzaldehyde (91.5 mg, 0.75 mmol). Control chromopohre was obtained as a blue solid (60 mg, yield 33%). ^{1}H NMR (400 MHz, DMSO-d_6): δ (ppm) 1.25-1.28 (t, J = 8.0 Hz, 6H), 1.86 (t, J = 4.0 Hz, 2H), 2.86 (t, J = 4.0 Hz, 2H), 2.92 (t, J = 4.0 Hz, 2H), 3.71-3.72 (m, 4H), 7.23 (s, 1H), 7.37-7.39 (d, J = 8.0 Hz, 2H), 7.48-7.50 (d, J = 8.0 Hz, 1H), 7.90-7.92 (m, 2H), 8.53 (s, 1H). ^{13}C NMR (100 MHz, DMSO-d_6): δ (ppm) 13.02, 21.41, 26.84, 27.13, 39.33, 39.53, 49.06, 95.73, 103.50, 119.10, 119.66, 123.94, 125.81, 125.89, 128.22, 132.54, 134.20, 148.95, 151.15, 151.23, 153.56, 153.64, 156.44, 158.99, 161.93. ^{19}F NMR (400 MHz, DMSO-d_6): δ (ppm) -131.76, -131.79. ESI-MS: m/z calcd for Control chromopohre ($C_{24}H_{24}F_2NO_2^+$, [M-ClO_4^-]$^+$), 396.18; found 396.25.

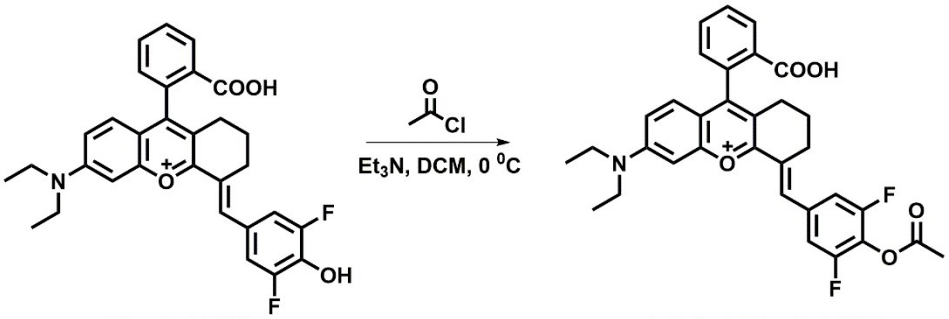

Rhodol-NIR acetylated Rhodol-NIR

Acetylated Rhodol-NIR: Compound Rhodol-NIR (133 mg, 0.21 mmol) and triethylamine (58 μL, 0.42 mmol) were dissolved in dichloromethane, and the mixture was stirred at 0 °C for 30 min under nitrogen. Then acetyl chloride (74.6 μL, 1.05 mmol) was dropwise added to the mixture. Then the mixture was stirred overnight. After the reaction was completed, the solvent was removed under reduced pressure to give the crude product, which was purified by silica gel flash chromatography using CH_2Cl_2 to CH_2Cl_2/ethanol (200:1 to 100:1) as eluent to afford compound acetylated Rhodol-NIR as a purple solid (55.2 mg, yield 40%). ^{1}H NMR (400 MHz, DMSO-d_6): δ (ppm) 1.08-1.11 (t, J=4.0 Hz, 6H), 1.54-1.61 (m, 2H), 1.85-1.89 (m, 2H), 2.41 (s, 3H), 2.59-2.77 (m, 2H), 3.32-3.35 (m, 4H), 6.38-6.51 (m, 3H), 7.30-7.37 (m, 4H), 7.66-7.69 (t, J= 8.0 Hz, 1H), 7.77-7.81 (t, J = 8.0 Hz, 1H), 7.93-7.95 (d, J=8.0 Hz, 1H). ^{13}C NMR (100 MHz, DMSO-d_6): δ (ppm) 12.83, 20.22, 22.22, 26.85, 97.19, 104.48, 109.47, 109.75, 113.49, 113.54, 113.66, 113.71, 122.86, 124.01, 125.08, 127.08, 128.67, 130.39, 132.91, 135.78, 136.44, 136.54, 136.63, 146.11, 149.49, 151.99, 153.28, 153.33, 155.75, 155.80, 168.04, 169.43. ^{19}F NMR (400 MHz, DMSO-d_6): δ (ppm) -127.07, -127.04. ESI-MS: m/z calcd for acetylated Rhodol-NIR ($C_{33}H_{29}F_2NO_5$, [M]), 557.2; found, 558.2

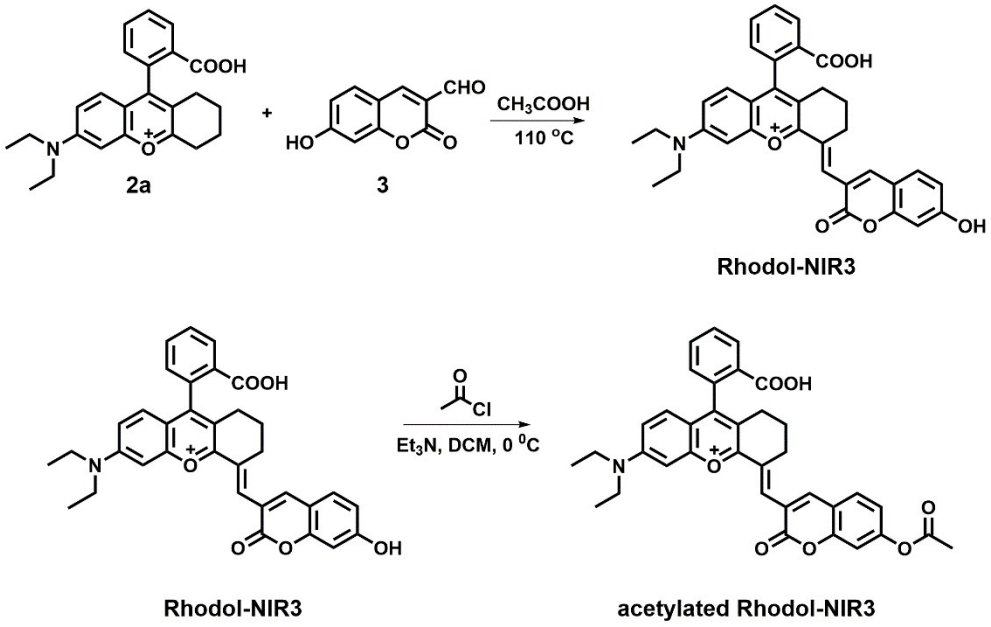

Rhodol-NIR3: Compound 3 was synthesized according to the literature.[S4] Compound 2a (178.1 mg, 0.5 mmol) and 3 (141.8 mg, 0.75 mmol) were dissolved in acetic acid (10 mL), and the reaction mixture was heated to 110 °C overnight. The solvent was removed under reduced pressure to give the product, which was purified by silica gel flash chromatography (CH_2Cl_2/MeOH, 200/1 to 20/1) to obtain Rhodol-NIR3 as a blue solid (64.8 mg, yield 20%). ESI-MS: m/z calcd for Rhodol-NIR3 ($C_{34}H_{30}NO_6^+$, $[M\text{-}ClO_4^-]^+$), 548.21; found 548.30.

Acetylated Rhodol-NIR3: Compound Rhodol-NIR3 (34 mg, 0.05 mmol) and triethylamine (14 μL, 0.1 mmol) were dissolved in dichloromethane, and the mixture was stirred at 0 °C for 30 min under nitrogen. Then acetyl chloride (18.6 μL, 0.25 mmol) was dropwise added and the mixture was stirred overnight. Afterward, the solvent was removed under reduced pressure to give the crude product, which was purified by silica gel flash chromatography using CH_2Cl_2 to CH_2Cl_2/ethanol (200:1 to 30:1) as eluent to afford acetylated Rhodol-NIR3 as a purple solid (27.6 mg, yield 80%). ESI-MS: m/z calcd for acetylated Rhodol-NIR3 ($C_{36}H_{32}NO_7^+$, $[M\text{-}ClO_4^-]^+$), 590.22; found 590.35.

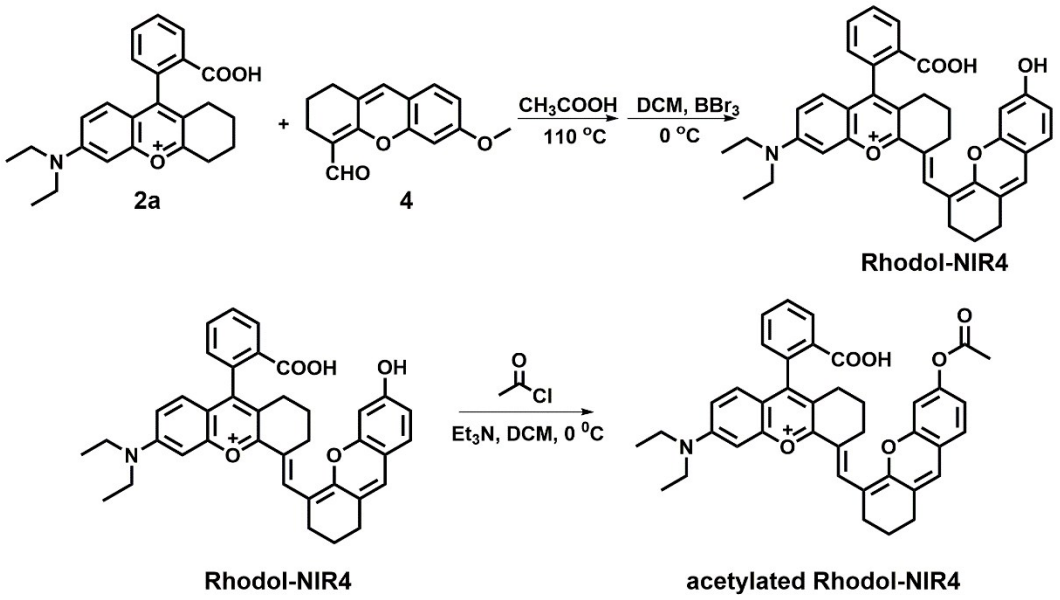

Rhodol-NIR4: Compound 4 was synthesized according to literature.[S5] Compound 2a (178.1 mg, 0.5 mmol) and 4 (181.5 mg, 0.75 mmol) were dissolved in acetic acid (10 mL), and the reaction mixture was heated to 110 °C overnight. The solvent was removed under reduced pressure. Then BBr_3 (20 eq) was dropwise added to the mixture at 0 °C and the mixture was stirred at 25 °C overnight. After the reaction was completed, saturated solution of $NaHCO_3$ was added at 0 °C, followed by extraction of the aqueous layer with CH_2Cl_2. The organic layer was then dried over Na_2SO_4, filtered and concentrated in vacuo. The residue was purified by silica gel flash chromatography (CH_2Cl_2/MeOH, 200/1 to 10/1) to obtain Rhodol-NIR4 as a blue solid (72 mg, yield 21%). ESI-MS: m/z calcd for Rhodol-NIR4 ($C_{38}H_{36}NO_5^+$, [M-ClO_4^-]$^+$), 586.26 found 586.32.

Acetylated Rhodol-NIR4 Compound Rhodol-NIR4 (34.3 mg, 0.05 mmol) and triethylamine (14 μL, 0.1 mmol) were dissolved in dichloromethane, and the mixture was stirred at 0 °C for 30 min. Then acetyl chloride (18.6 μL, 0.25 mmol) was dropwise added to the mixture and stirred overnight. After the reaction was completed, the solvent was removed under reduced pressure to give the crude product, which was purified by silica gel flash chromatography (CH_2Cl_2/MeOH, 200/1 to 20/1) to afford acetylated Rhodol-NIR4 as a purple solid (27.6 mg, yield 82%). ESI-MS:

m/z calcd for acetylated Rhodol-NIR4 ($C_{40}H_{38}NO_6^+$, $[M\text{-}ClO_4^-]^+$), 628.27; found 628.27.

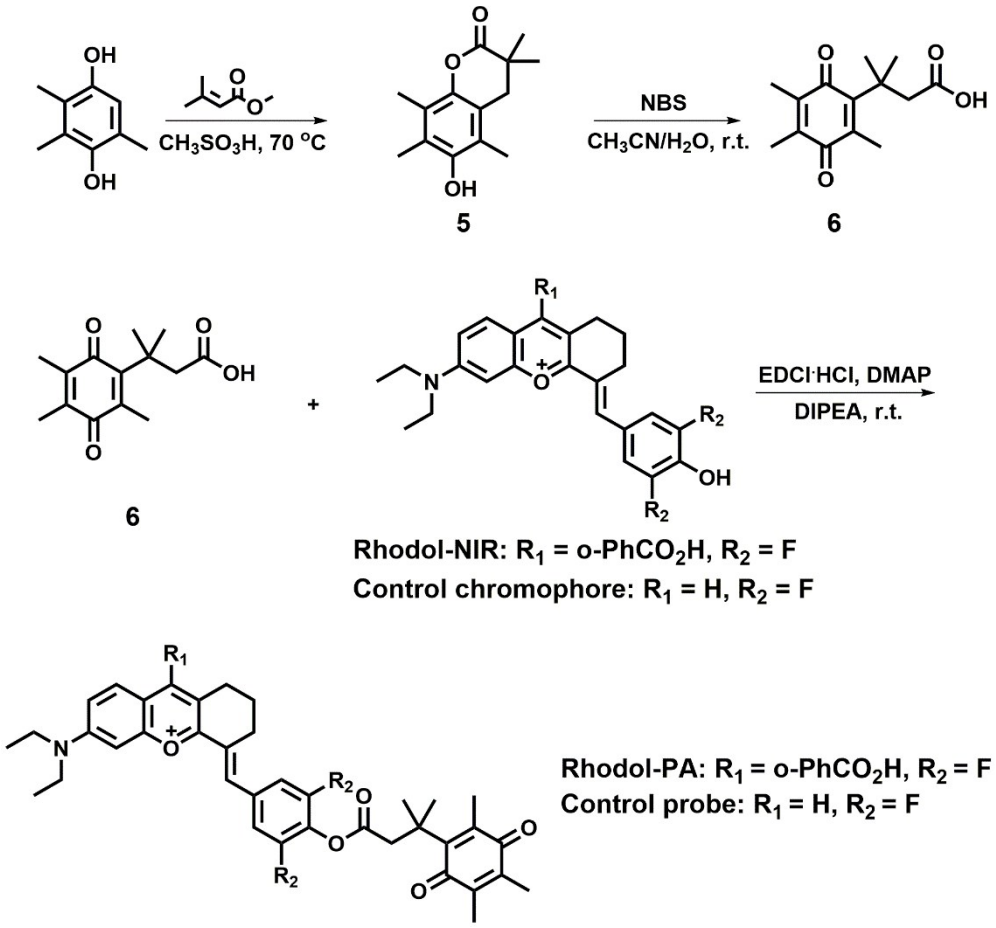

Compound 5 and compound 6 were prepared according to literature with slight modifications.[S6]

Rhodol-PA: Rhodol-NIR (234.0 mg, 0.38 mmol) was slowly added to a solution of 1-(3-dimethylaminopropyl)-3-ethylcarbodiimide hydrochloride (72.8 mg, 0.38 mmol), compound 4 (167.3 mg, 0.58 mmol), and 4-dimethylaminopyridine (46.4 mg, 0.38 mmol) in CH_2Cl_2 (30 mL) at 0 °C. After reacting for 12 h, the mixture was washed with HCl (1 M). The organic layer was dried with $MgSO_4$, filtered and concentrated under vacuum. The residues were purified by silica gel column chromatography using CH_2Cl_2/MeOH (100 : 1 to 20 : 1) as eluents to obtain Rhodol-PA as a purple solid (164.7 mg, yield 58%). ^{1}H NMR (400 MHz, CD_3Cl): δ (ppm) 1.16-1.19 (t, J = 4.0 Hz, 6H), 1.26-1.31 (m, 2H), 1.55 (s, 6H), 1.65 (s, 3H), 1.94 (s, 3H), 1.96 (s, 3H), 2.04-2.07 (m, 2H), 2.18 (s, 3H), 2.55-2.76 (m, 2H), 3.35-3.37 (m, 4H), 6.39-6.52 (m, 3H),

6.95-6.98 (d, J = 12.0 Hz, 2H), 7.21-7.23 (d, J = 8.0 Hz, 2H), 7.54-7.7.58 (t, J = 8.0 Hz, 1H), 7.63-7.67 (t, J = 8.0 Hz, 1H), 7.95-7.97(d, J=8.0 Hz, 2H). ^{13}C NMR (100 MHz, CD_3Cl): δ (ppm) 12.19, 12.54, 14.31, 22.20, 22.98, 27.08, 28.97, 38.54, 46.95, 86.68, 97.18, 112.75, 112.97, 122.69, 122.72, 122.74, 123.55, 125.19, 127.57, 128.65, 129.41, 132.73, 134.54, 136.26, 136.35, 138.69, 139.56, 142.90, 151.31, 152.00, 152.21, 153.38, 155.87, 169.49, 169.91, 187.45, 190.69. ^{19}F NMR (400 MHz, DMSO-d_6): δ (ppm) -127.06, -127.04. HRMS (ESI): m/z calcd for Rhodol-PA ($C_{45}H_{43}F_2NO_7$, [M]), 747.3008; found, 748.3098.

Control probe: Control probe, prepared similarly as Rhodol-PA using Control choromopore (213.3 mg, 0.43 mmol), 1-(3-dimethylaminopropyl)-3-ethylcarbodiimide hydrochloride (165 mg, 0.86 mmol), Compound 4 (300 mg, 0.58 mmol) and DMAP (53 mg, 0.43 mmol), was obtained as a purple solid (187.8 mg, yield 60%). ^{1}H NMR (400 MHz, CD_3Cl): δ (ppm) 1.37 (s, 6H), 1.55 (s, 6H), 1.92-1.95 (m, 8H), 2.18 (s, 3H), 2.89-2.94 (m, 4H), 2.89-2.94 (d, 3H), 3.35 (s, 2H), 3.72-3.73 (m, 4H), 5.31(s, 1H), 7.21-7.25 (m, 3H),7.86-7.88 (d, J=8.0 Hz, 1H), 7.99 (s, 1H), 8.33 (s, 1H). ^{13}C NMR (100 MHz, CD_3Cl): δ (ppm) 12.17, 12.52, 14.30, 21.42, 26.94, 27.28, 28.96, 29.58, 38.52, 46.88, 96.21, 114.12, 114.34, 118.86, 120.44, 123.73, 129.80, 132.67, 133.66, 138.73, 139.68, 142.82, 148.69, 153.44, 153.49, 155.93, 155.98, 156.88, 159.22, 161.24, 169.17, 177.17, 187.38, 190.58. ^{19}F NMR (400 MHz, CD_3Cl): δ (ppm) -124.63, -124.61. HRMS (ESI): m/z calcd for Control probe ($C_{38}H_{40}F_2NO_2^+$, $[M]^+$), 628.2869; found, 628.2870.

References

S1. D. Magde, J. H. Brannon, T. L. Cremers and J. Olmsted, *J. Phys. Chem.,* 1979, **83**, 696-699.

S2. M. J. Frisch, G. W. Trucks, H. B. Schlegel, G. E. Scuseria, M. A. Robb, J. R. Cheeseman, G. Scalmani, V. Barone, B. Mennucci, G. A. Petersson, H. Nakatsuji, M. Caricato, X. Li, H. P. Hratchian, A. F. Izmaylov, J. Bloino, G. Zheng, J. L. Sonnenberg, M. Hada, M. Ehara, K. Toyota, R. Fukuda, J. Hasegawa, M. Ishida, T. Nakajima, Y. Honda, O. Kitao, H. Nakai, T. Vreven, J. A. Montgomery, J. E. Peralta, F. Ogliaro, M. Bearpark, J. J. Heyd, E. Brothers, K. N. Kudin, V. N. Staroverov, R. Kobayashi, J. Normand, K. Raghavachari, A. Rendell, J. C. Burant, S. S. Iyengar, J. Tomasi, M. Cossi, N. Rega, J. M. Millam, M. Klene, J. E. Knox, J. B. Cross, V. Bakken, C. Adamo, J. Jaramillo, R. Gomperts, R. E. Stratmann, O. Yazyev, A. J. Austin, R. Cammi, C. Pomelli, J. W. Ochterski, R. L. Martin, K. Morokuma, V. G. Zakrzewski, G. A. Voth, P. Salvador, J. J. Dannenberg, S. Dapprich, A. D. Daniels, O. Farkas, J. B. Foresman, J. V. Ortiz, J. Cioslowski, D. J. Fox, Gaussian, Inc., Wallingford CT, Gaussian 09, Revision B.01, 2010.

S3. L. Yuan, W. Y. Lin, Y. Yang and H. Chen, *J. Am. Chem. Soc.,* 2012, **134**, 1200-1211.

S4. B.W. Li, P. L. Liu, H. Wu, X. Xie, Z. L. Chen, F. Zeng and S. Z. Wu, *Biomaterials,* 2017, **138**, 57-68.

S5. J. A. Richard, *Org. Biomol. Chem.,* 2015, **13**, 8169-8172.

S6. R. D. Rohde, H. D. Agnew, W. Seok. Yeo, R. C. Bailey and J. R. Heath, *J. Am. Chem. Soc.,* 2006, **128**, 9518-9525.

Fig. S1 Fluorescence emission spectra of Rhodol-NIR, Rhodol-NIR1 and Rhodol-NIR2 (15 μM) at pH 7.4. λ_{ex}= 620 nm.

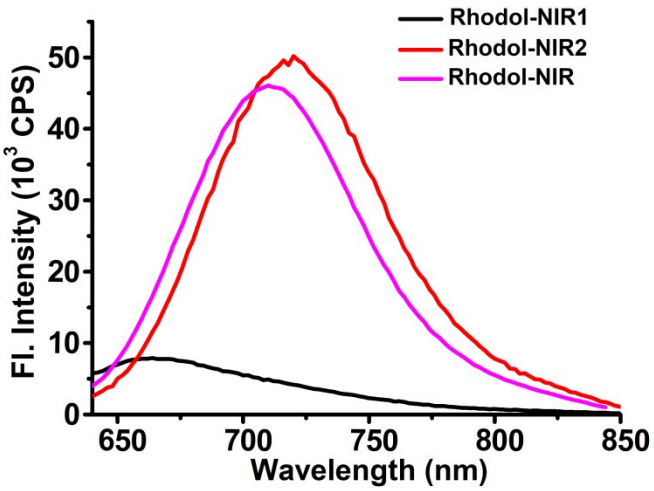

Fig. S2 Acid-base equilibrium and pH-dependence of absorption and fluorescence spectra of Rhodol-NIR1 in buffers of various pH values, containing 0.5% DMSO as a cosolvent. Excitation wavelength was 650 nm. Absorbance at 650 nm and fluorescence intensity at 720 nm were used to plot the pH profile. The pKa of the phenolic hydroxyl moiety of Rhodol-NIR1 was calculated to be 8.7.

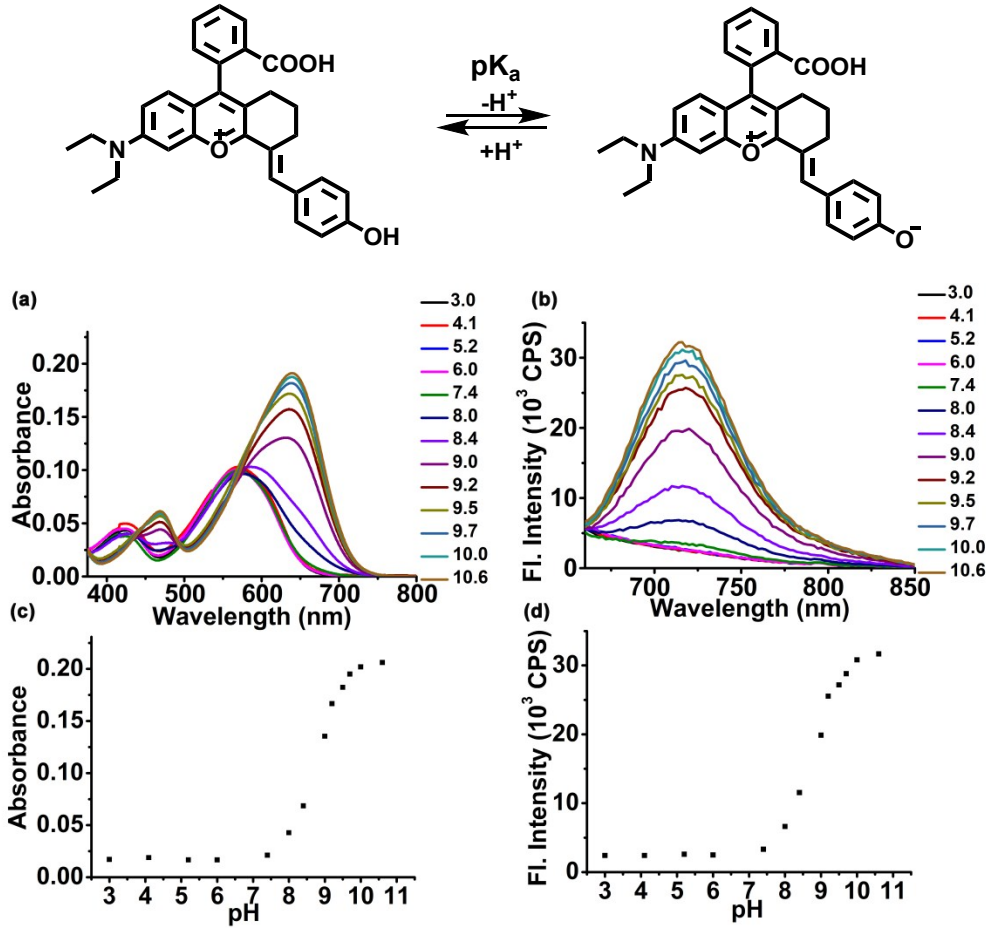

Fig. S3 Acid-base equilibrium and pH-dependence of absorption and fluorescence spectra of Rhodol-NIR in buffers of various pH values, containing 0.5% DMSO as a cosolvent. Excitation wavelength was 620 nm. Absorbance at 650 nm and fluorescence intensity at 720 nm were used to plot the pH profile. The pKa of the phenolic hydroxyl moiety of Rhodol-NIR was calculated to be 6.1.

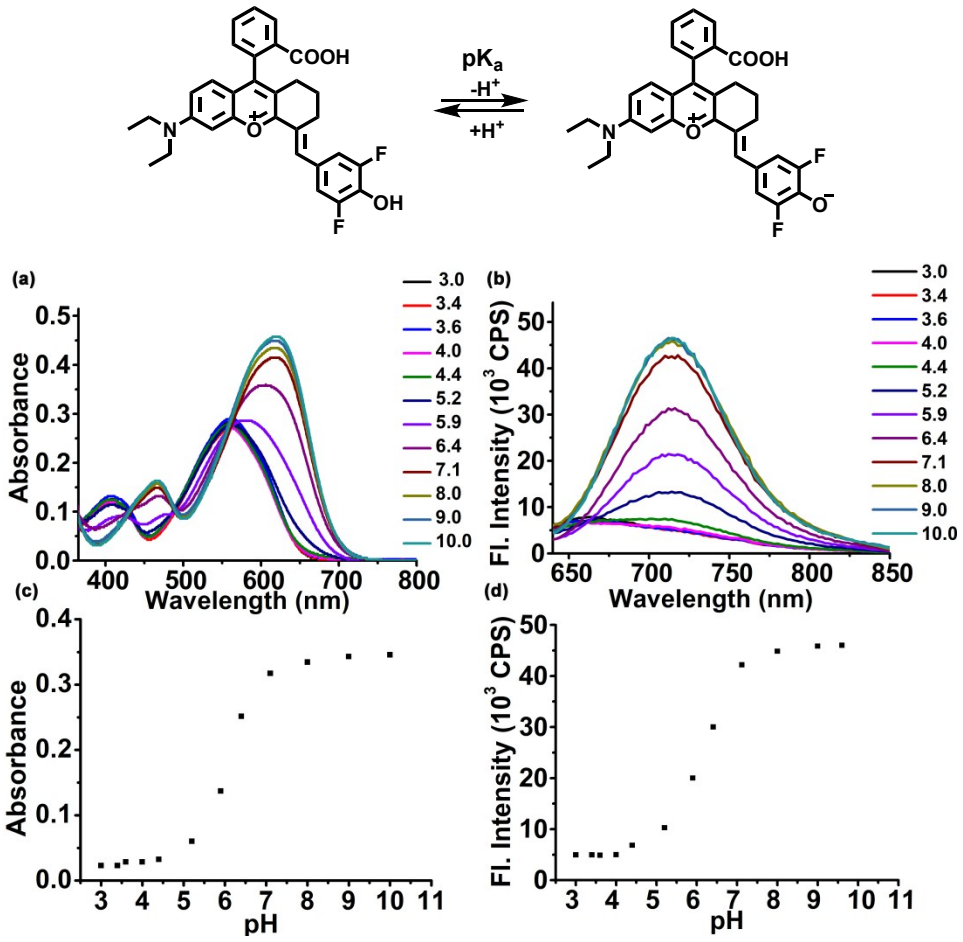

Fig. S4 Acid-base equilibrium and pH-dependence of absorption and fluorescence spectra of Rhodol-NIR2 in buffers of various pH values, containing 0.5% DMSO as a cosolvent. Excitation wavelength was 620 nm. Absorbance at 650 nm and fluorescence intensity at 720 nm were used to plot the pH profile. The pKa of the phenolic hydroxyl moiety of Rhodol-NIR2 was calculated to be 6.4.

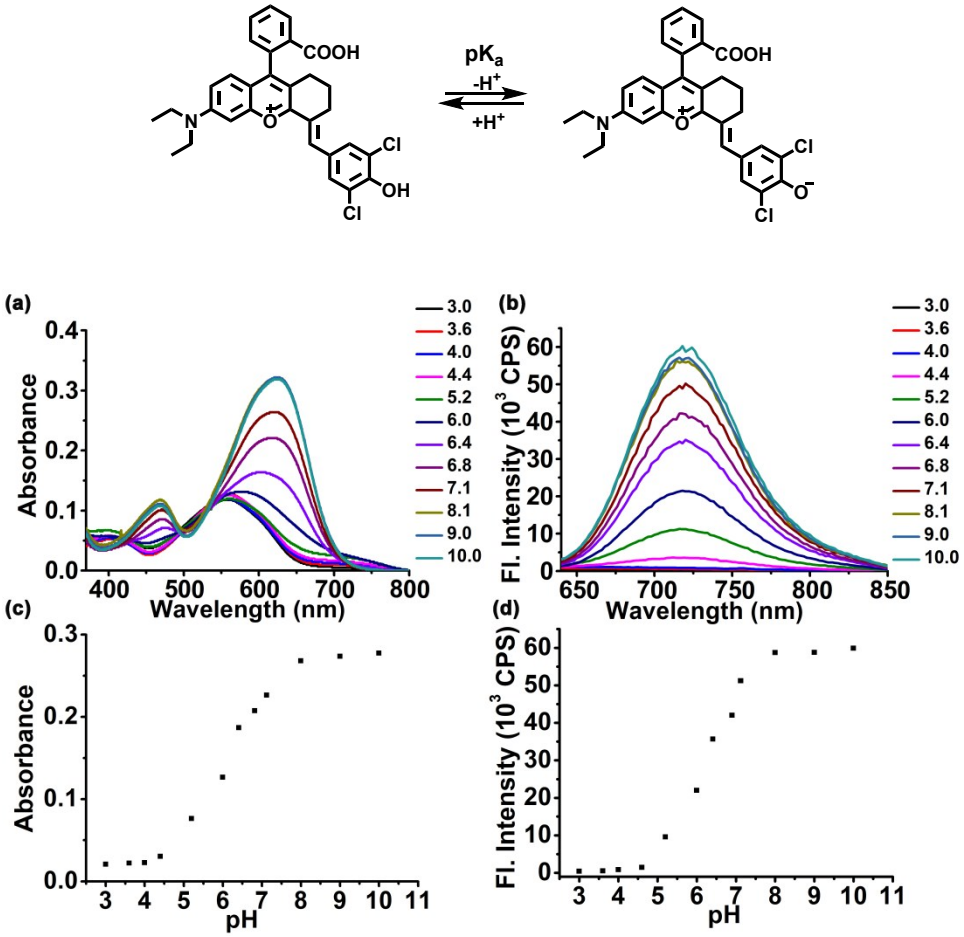

Fig. S5 Photostability investigation of Rhodol-NIR using ICG as the reference. Fluorescence intensity of Rhodol-NIR (15 μM) and ICG (15 μM) at different time points during extended exposure to a mercury lamp in PBS buffer (10 mM, pH = 7.4, containing 0.5% DMSO).

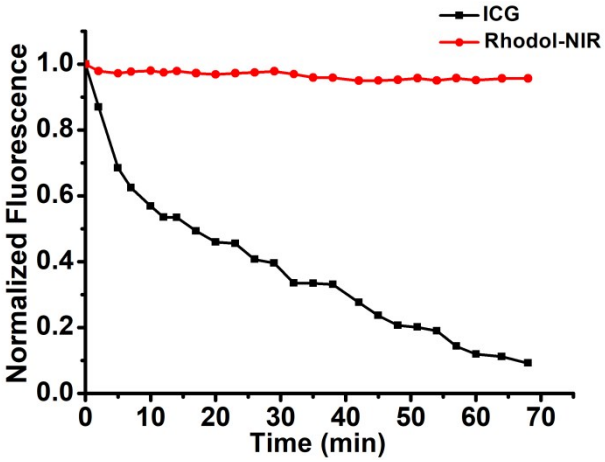

Fig.S6 (a) UV-Vis absorption spectra of Rhodol-NIR3 and acetylated Rhodol-NIR3 (15 μM) at pH 7.4; (b) UV-Vis absorption spectra of Rhodol-NIR4 and acetylated Rhodol-NIR4 (15 μM) at pH 7.4.

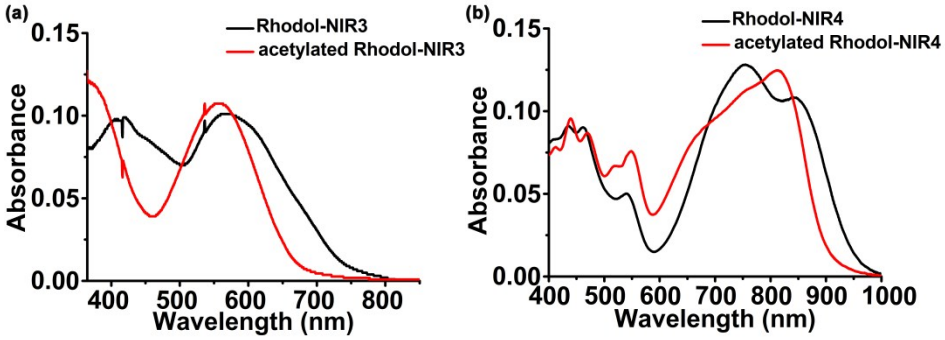

Fig.S7 For Rhodol-NIR1 and Rhodol-NIR, we chose their phenoate forms, resonance structures of the dissociated hydroxyl phenolic forms, for theoretical calculations as we have demonstrated that Rhodol-NIR1 and Rhodol-NIR were predominately present in the spirocyclic ring-open form structure. For acetylated Rhodol-NIR, the closed spirolactone structure was chosen for theoretical calculations. DFT optimized ground-state geometry (S0) and molecular orbital plots (LUMO and HOMO) of different compounds in water. Carbon, nitrogen, oxygen, chlorine and fluorin atoms are colored in gray, blue, red, green, respectively, in the ball-and-stick representation.

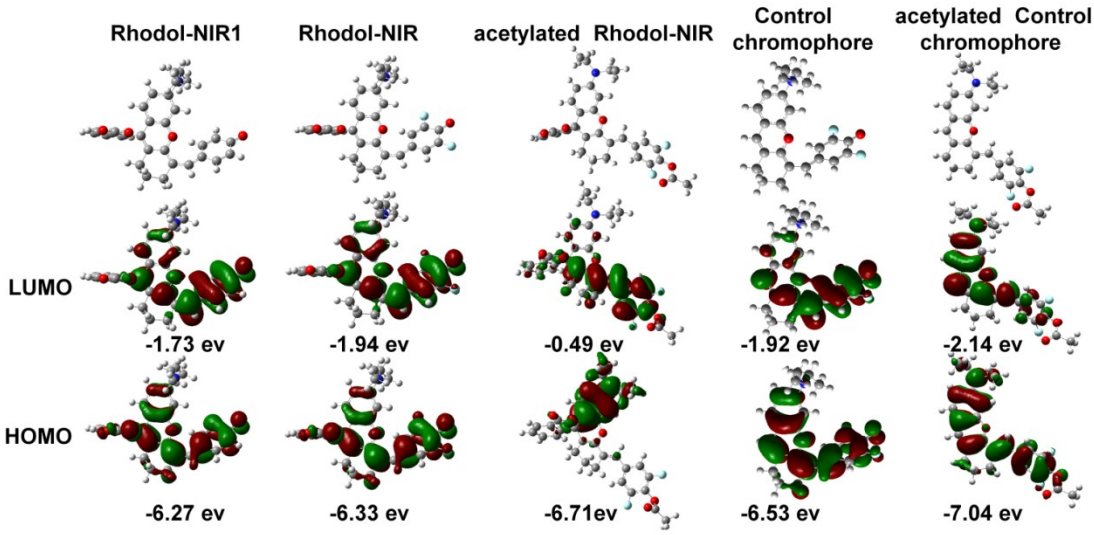

Table S1. Summary of photophysical properties

Compound	λ_{abs}(nm)[1]	λ_{em}(nm)[2]	pK_a	ε_{max} [3]	Absorption Ratio[4]	ΔE(eV)[5]
Rhodol-NIR1	570	663	8.7	6.81×10^4	--	4.54
Rhodol-NIR2	630	720	6.4	1.79×10^5	--	--
Rhodol-NIR	630	718	6.1	2.69×10^5	--	4.39
Rhodol-PA	300	--	--	--	57	6.22*
Control probe	550	--	--	9.93×10^4	3	4.90**

[1] absorption maximum, [2] emission maximum, [3] molar extinction coefficient. Units: M^{-1} cm^{-1}, [4] ratio of absorbance at 630 nm after to before enzymatic reaction, [5] HOMO-LUMO energy gap, *acetylated Rhodol-NIR, **acetylated Control chromophore.

Table S2. HOMO and LUMO energies of rhodol variants based on TDDFT B3LYP/6-31G* calculation.

Compound	HOMO (eV)	LUMO (eV)	λ_{abs} (nm) Calculation	λ_{abs} (nm) Experiment	Eletronegativity[a]
Rhodol-NIR1	-6.27	-1.73	537	650	-0.58
Rhodol-NIR	-6.33	-1.94	557	630	-0.53
Acetylated Rhodol-NIR	-6.71	-0.49	286	--	--
Control chromopohre	-6.53	-1.92	523	610	--
Acetylated Control chromopohre	-7.04	-2.14	452	550	--

[a] Electronegativity for the oxygen atom of phenolic hydroxyl moiety.

Fig. S8 HPLC chromatogram of Rhodol-NIR, Rhodol-PA and the reaction products of Rhodol-PA and hNQO1 (3.0 μg mL^{-1}) in the presence of NADH (100 μM). Detection wavelength: 550 nm.

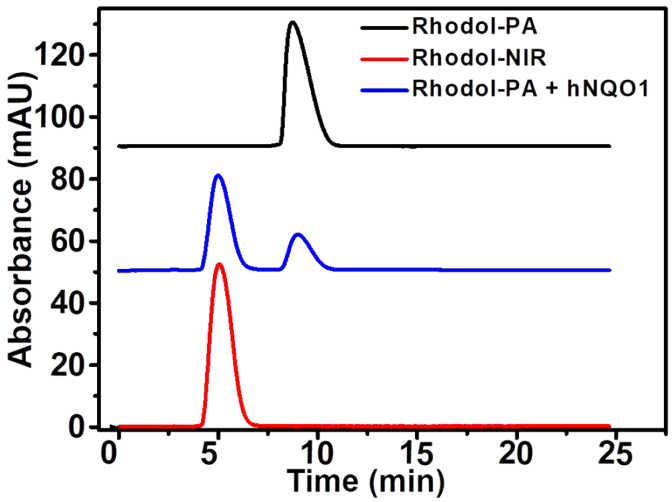

Fig. S9 HRMS-ESI spectra of the reaction products of Rhodol-PA (15 μM) toward hNQO1 (1.5 μg/mL).

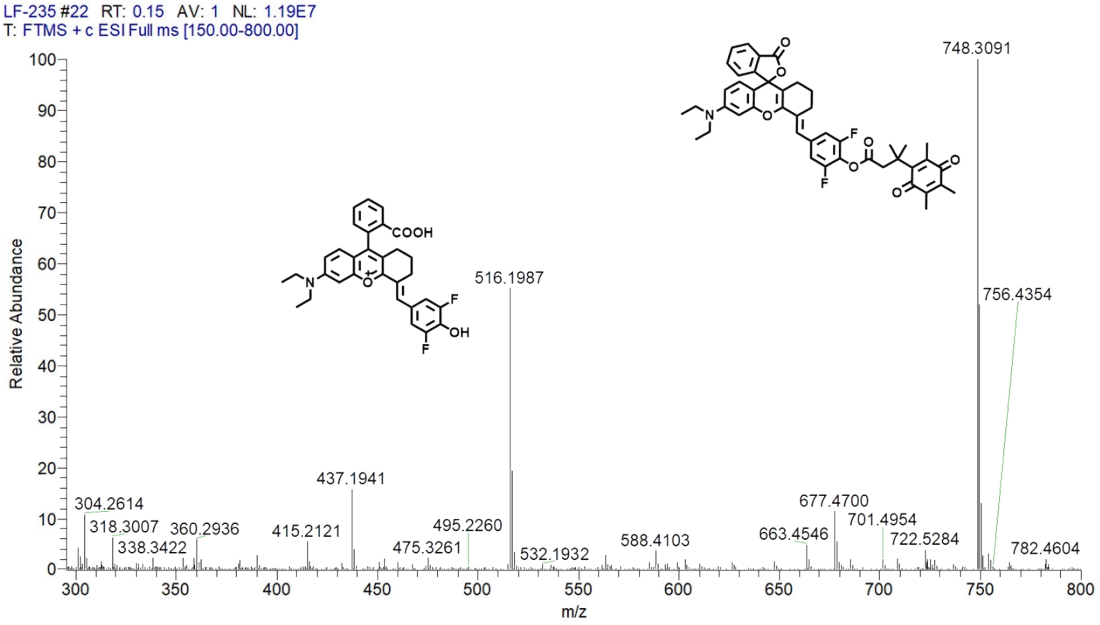

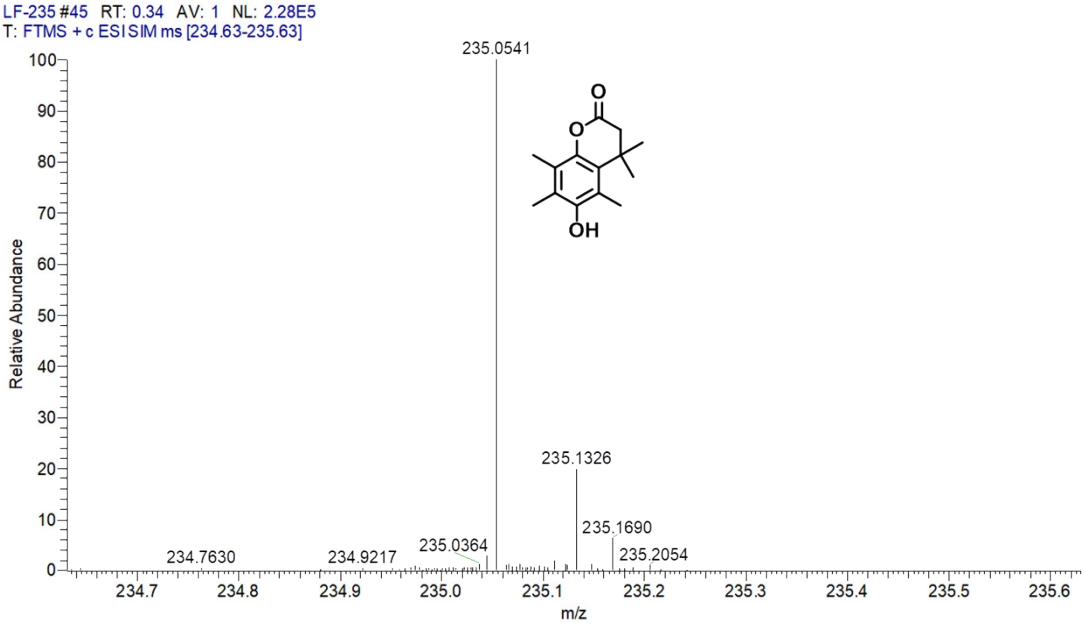

Fig. S10 (a) Fluorescence spectra of Rhodol-PA and Control probe (15 μM) in the absence or presence of hNQO1 (3.0 μg/mL^{-1}) at 37 °C in PBS buffer (10 mM, pH = 7.4, containing 0.5% DMSO) for 1.5 h. Excitation: 620 nm. (b) Photographs of Rhodol-PA and Control probe (15 μM) in response to hNQO1 (3.0 μg/mL^{-1}).

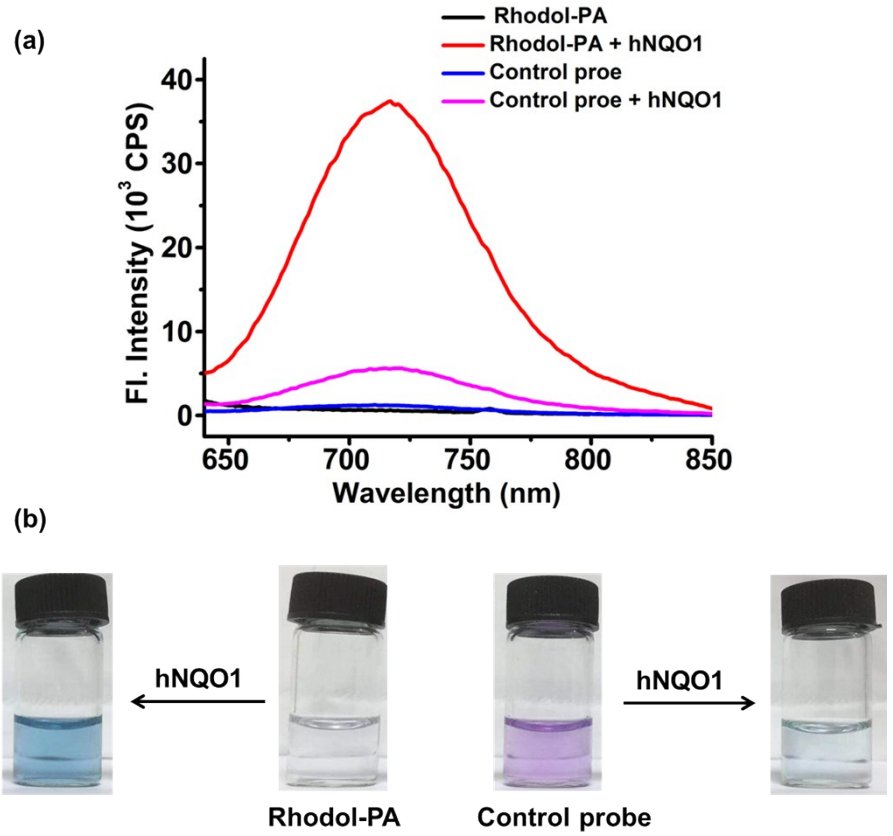

Fig. S11 Selectivity of Rhodol-PA (15 μM) towards various relevant substanaces based on PA (a) and fluorescence (b), $\lambda_{ex/em}$ = 620/720 nm. Lysate 1 was from HT-29 cell (overexpression of hNQO1), lysate 2 was from HT-29 cells with inhibitor, and lysate 3 was from MDA-MB-231 cells (very low expression of hNQO1).

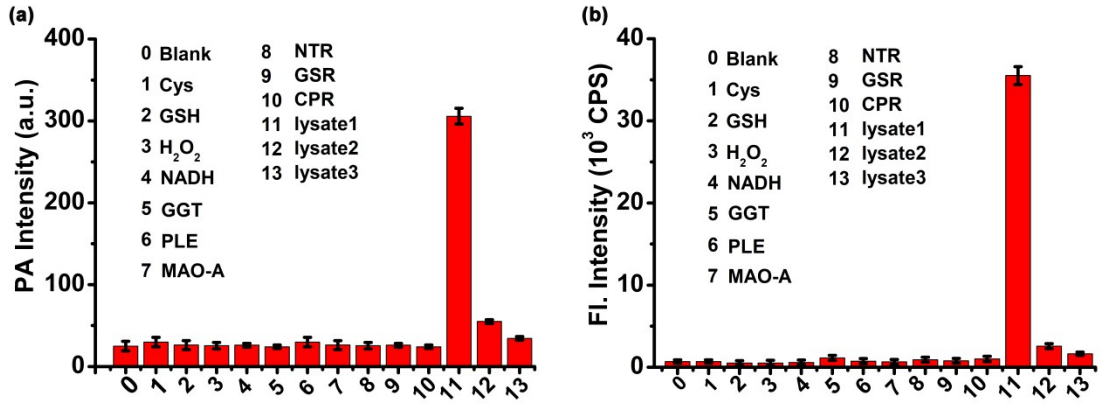

Fig. S12 UV-Vis absorption spectra (a) and fluorescence spectra (b) of Rhodol-PA (15 μM), Rhodol-PA (15 μM) + lysates of MDA-MB-231 cells (5 μL), Rhodol-PA (15 μM) + lysates of HT-29 cells (5 μL) + the inhibitor dicoumarol (100 μM), Rhodol-PA (15 μM) + lysates of HT-29 cells (5 μL) at 37 °C in PBS buffer (10 mM, pH = 7.4, containing 0.5% DMSO). λ_{ex}= 620 nm.

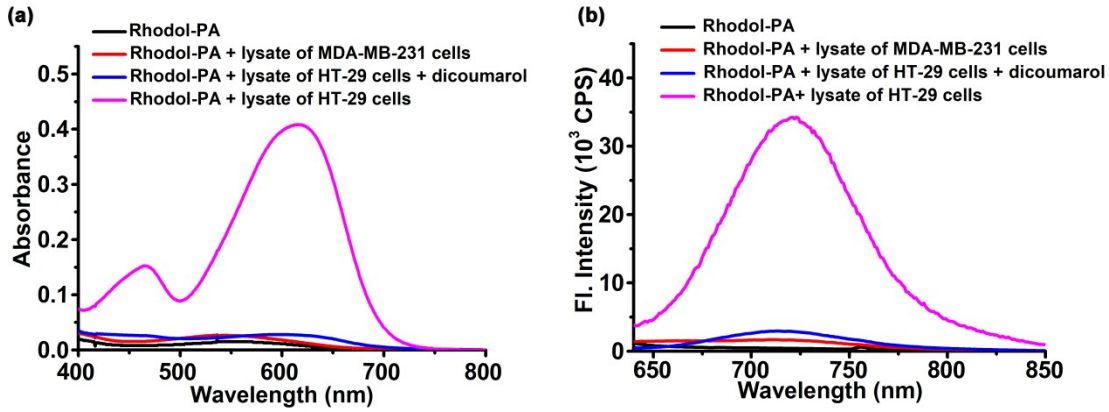

Fig. S13 (a) The linear fitting curve between the PA intensity (15 μM) and the concentrations of hNQO1 from 0.25 to 1.1 μg/mL. (b) Absorption (λ_{abs}=630 nm) of Rhodol-PA probe (15 μM) in response to different concentrations of hNQO1 in the presence of NADH (100 μM) in PBS (10 mM, pH = 7.4, containing 0.5% DMSO) at 37 °C. (c) The linear fitting curve between the absorption of Rhodol-PA (15 μM) and the concentrations of hNQO1 from 0.05 to 0.45 μg/mL. (d) Fluorescence intensities (λ_{em}= 720 nm) of Rhodol-PA probe (15 μM) in response to different concentrations of hNQO1. (e) The linear fitting curve between the fluorescence intensities of Rhodol-PA probe and the concentrations of hNQO1 from 0.05 to 0.45 μg/mL. Error bars represent the standard deviation (SD). Data were represented as mean ± SD.

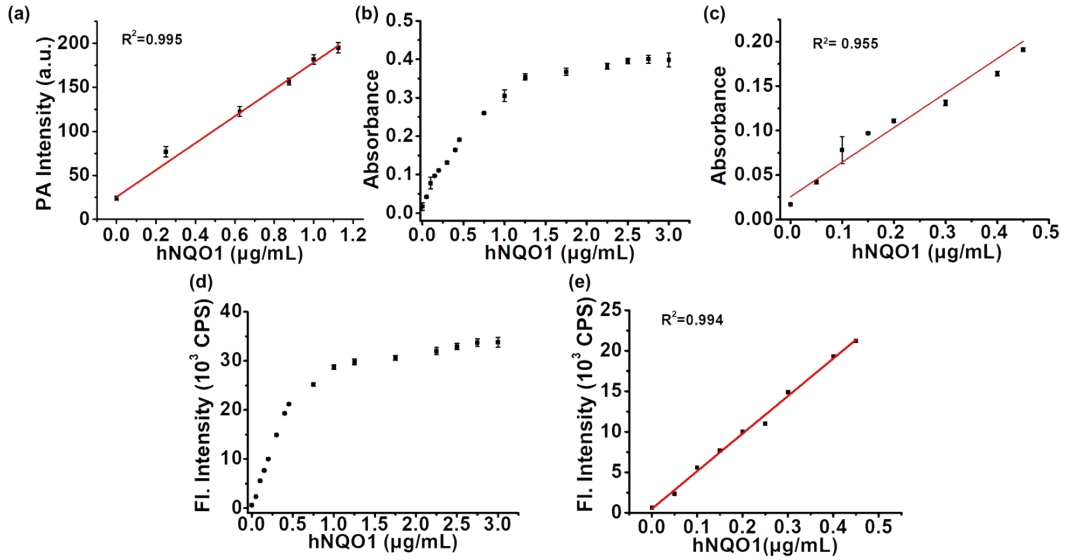

Fig. S14 Line weaver-Burk plot for the enzyme-catalyzed reaction. The Michaelis-Menten equation was described as: $V=V_{max}$ [probe] /(K_m + [probe]), where V is the reaction rate, [probe] is the concentration of Rhodol-PA (substrate), and K_m is the Michaelis constant. Conditions: 5.0 μg/mL hNQO1, 5-60 μM Rhodol-PA. $\lambda_{ex/em}$ = 620/720 nm. Each concentration was repeated three times, and the error bars represent standard deviations. Points were fitted using a linear regression model (correlation coefficient R^2 = 0.996).

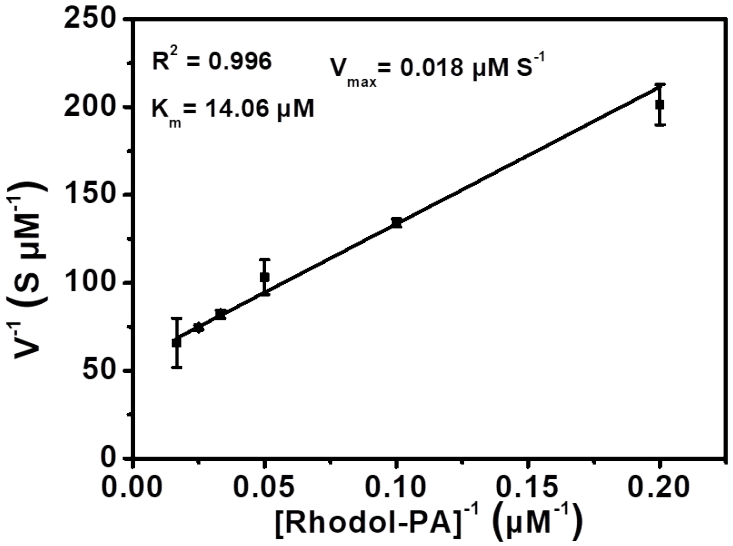

Fig. S15 Effect of pH value on fluorescence intensity of Rhodol-PA (15 μM) reacted with hNQO1 (3.0 μg/mL) in the presence of NADH (100 μM) at 37 °C.

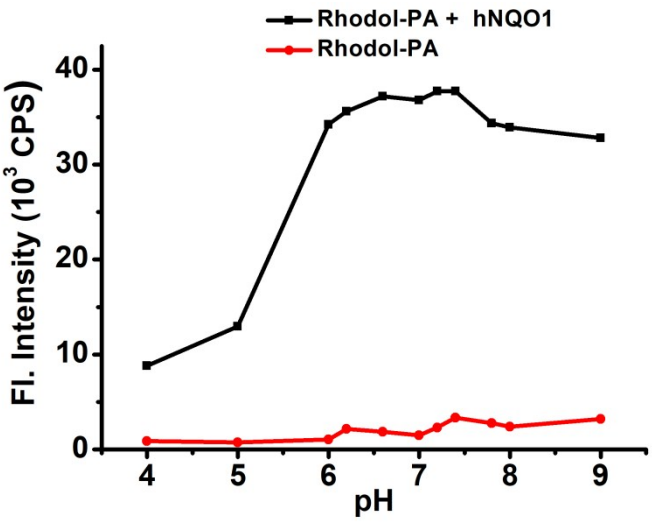

Fig. S16 (a) Confocal fluorescence images of HT-29 cells (overexpression of hNQO1) and MDA-MB-231 cells (very low expression of hNQO1) incubated with 20 μM Rhodol-PA for 1.5 h or pretreated with the inhibitor dicoumarol (100 μM) for 1 h and then incubated with 20 μM Rhodol-PA for 1.5 h. Scale bar =20 μm. (b) Quantification of fluorescence intensities of the MDA-MB-231 and HT-29 cells after incubation with Rhodol-PA in (a).

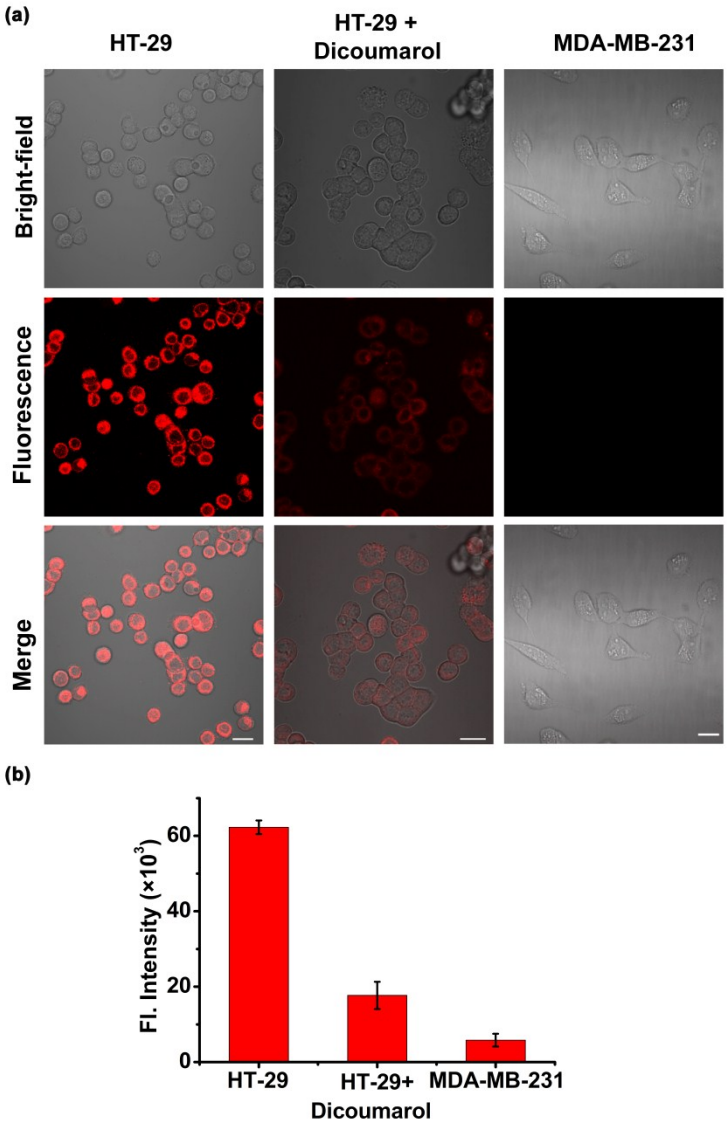

Fig. S17 Subcellular colocalization assays of Rhodol-PA with Hoechst 33342 (Hoechst), Mito-Tracker and Lyso-Tracker in HT-29 cells, respectively. Scale bar = 20 μm.

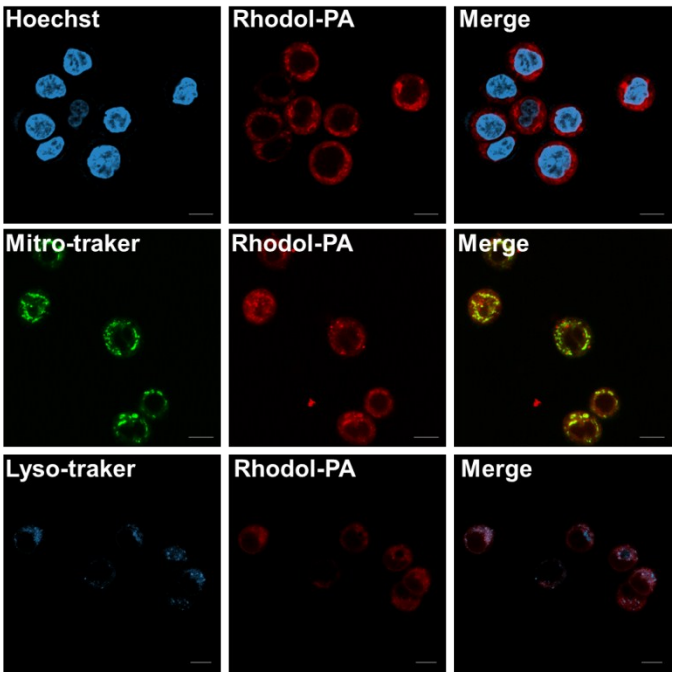

Fig. S18 Effects of Rhodol-PA (0 - 300 μM) on the viability of HT-29 cells and MDA-MB-231 cells, respectively. The viability of cells without Rhodol-PA is defined as 100%, The results are the means ± SD of three experiments.

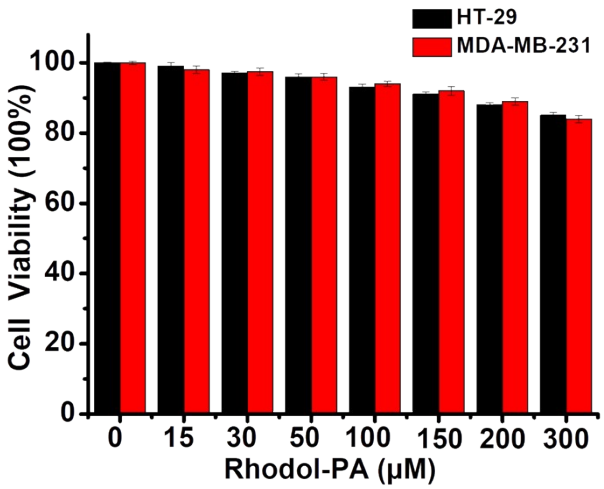

Fig. S19 (a) Representative PA images of HT-29 tumor-bearing mice (overexpression of hNQO1) at different time points upon tail vein injection of PBS. Dashed circles indicated the tumor area. Scale bars = 2 mm. (b) Time-dependent PA intensity of HT-29 tumor bearing mice upon injection of PBS (n = 3).

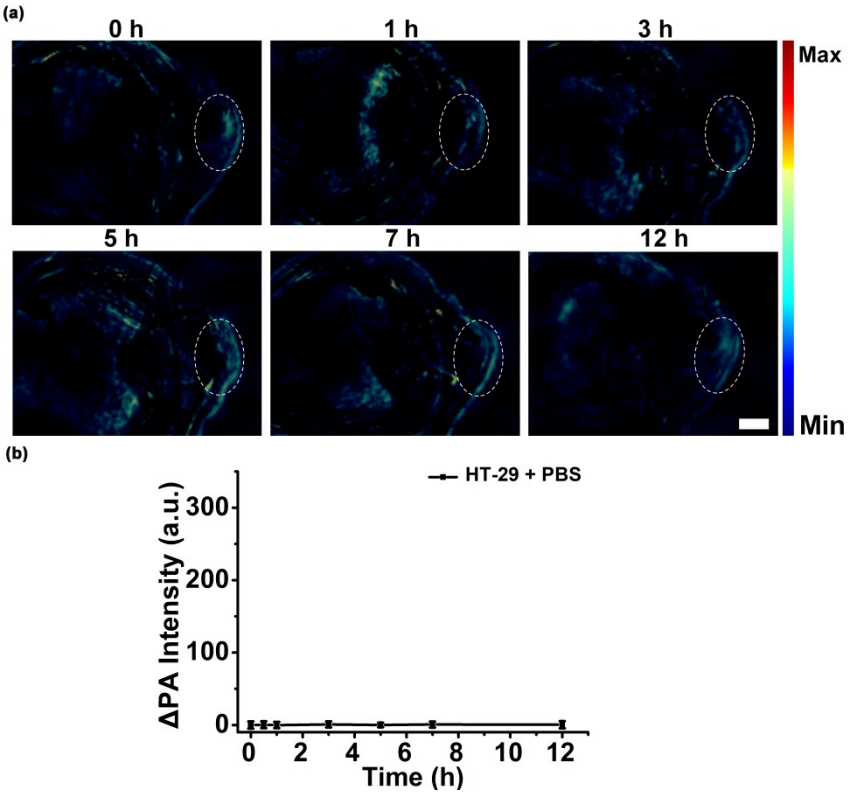

Fig. S20 (a) Representative *ex vivo* fluorescence images of organs and tumors dissected at 5 h post injection of Rhodol-PA from mice bearing HT-29 (overexpression of hNQO1) and MDA-MB-231 tumors (very low expression of hNQO1), respectively. (b) Quantitative fluorescence intensity of major organs (heart, liver, spleen, lung, and kidney) and tumors in HT-29 and MDA-MB-231 tumor-bearing mice at 5 h after tail vein injection of Rhodol-PA (mean ± SD, n = 3, $P < 0.05$).

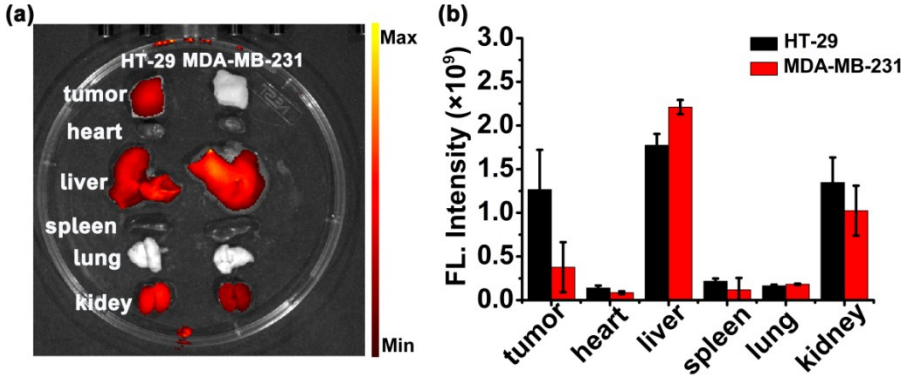

Fig. S21 (a) Representative *ex vivo* fluorescence image of organs and tumors excised from HT-29 tumor-bearing mice (overexpression of hNQO1) (b) Quantitative fluorescence intensity of major organs (heart, liver, spleen, lung, and kidney) and tumors in HT-29 tumor-bearing mice at different time points (0, 5, 12 and 24 h) after tail vein injection of Rhodol-PA (mean ± SD, n = 3).

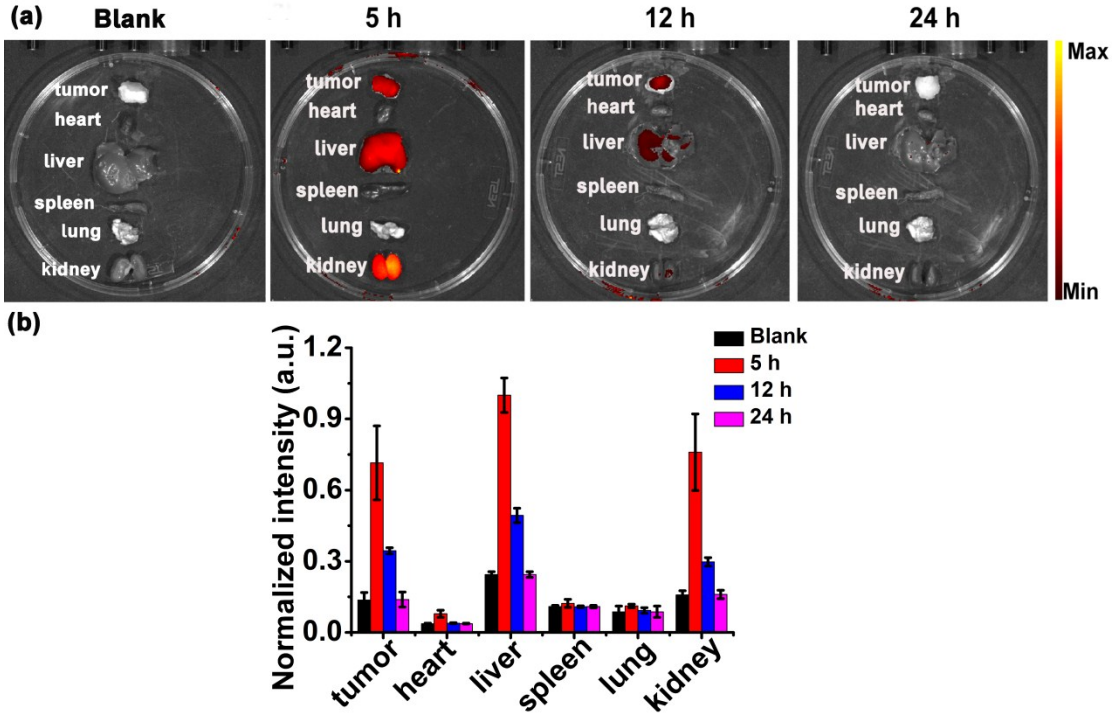

Fig. S22 ^{1}H NMR (400 MHz, CD_3OD) spectrum of Rhodol-NIR1.

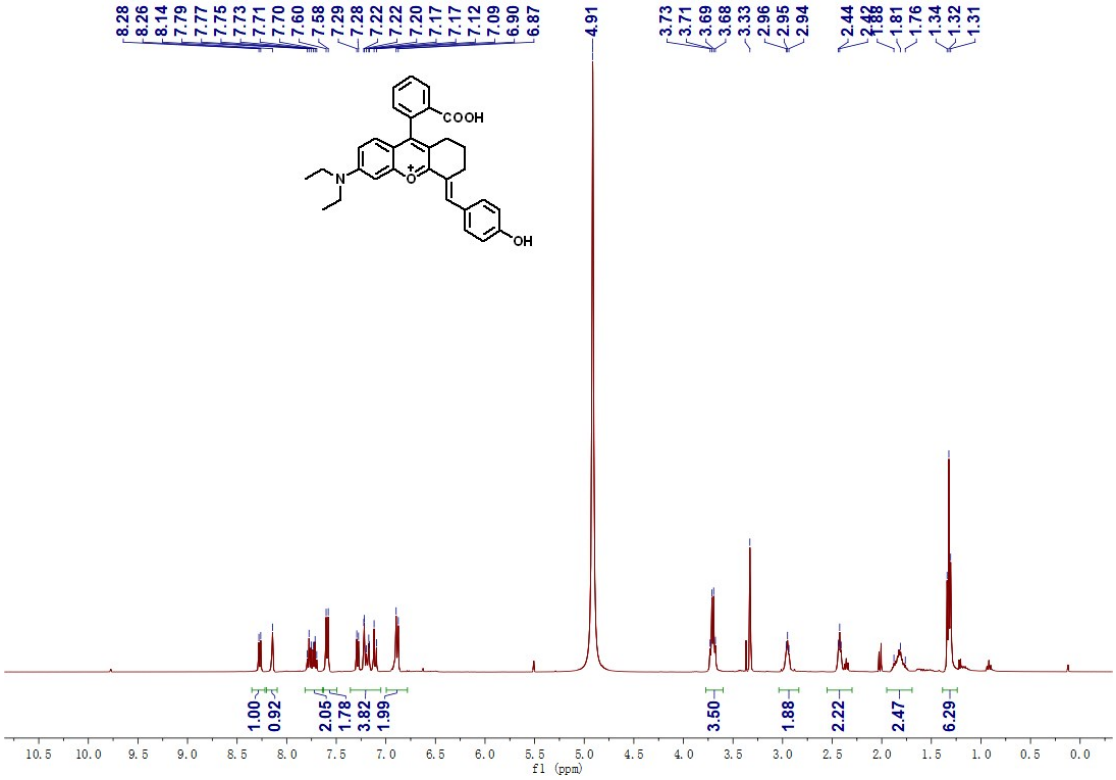

Fig. S23 ^{13}C NMR (400 MHz, CD_3OD) spectrum of Rhodol-NIR1.

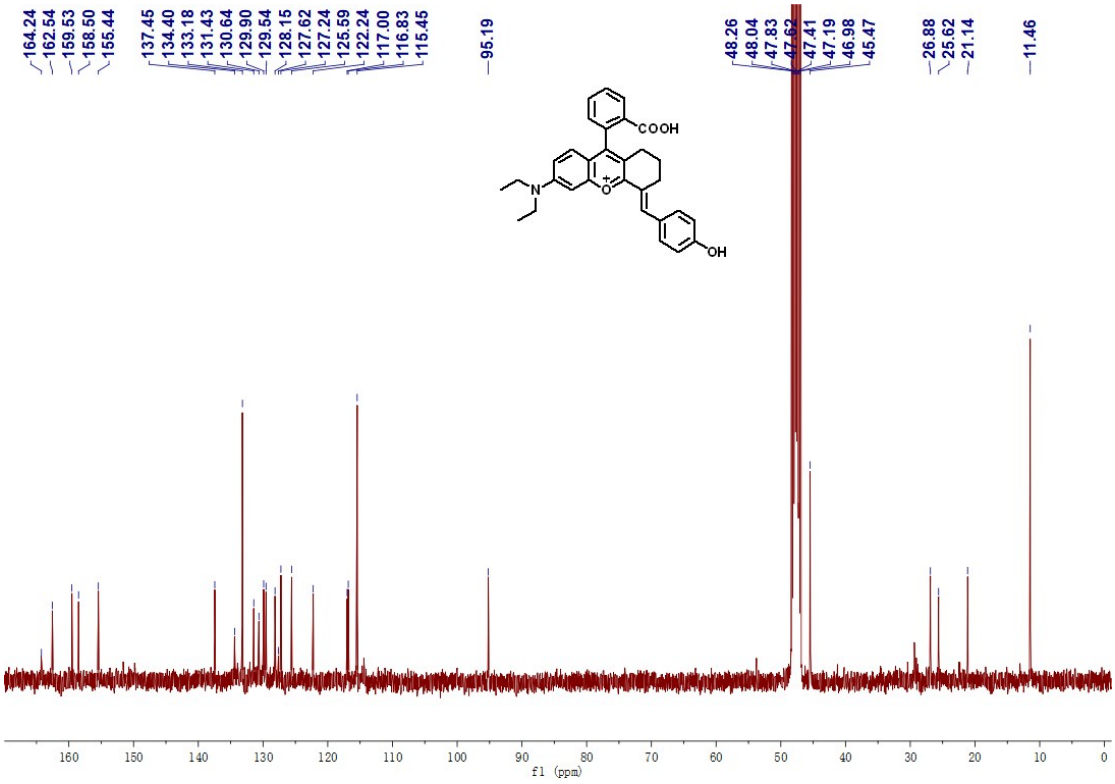

Fig. S24 ESI-MS spectrum of Rhodol-NIR1.

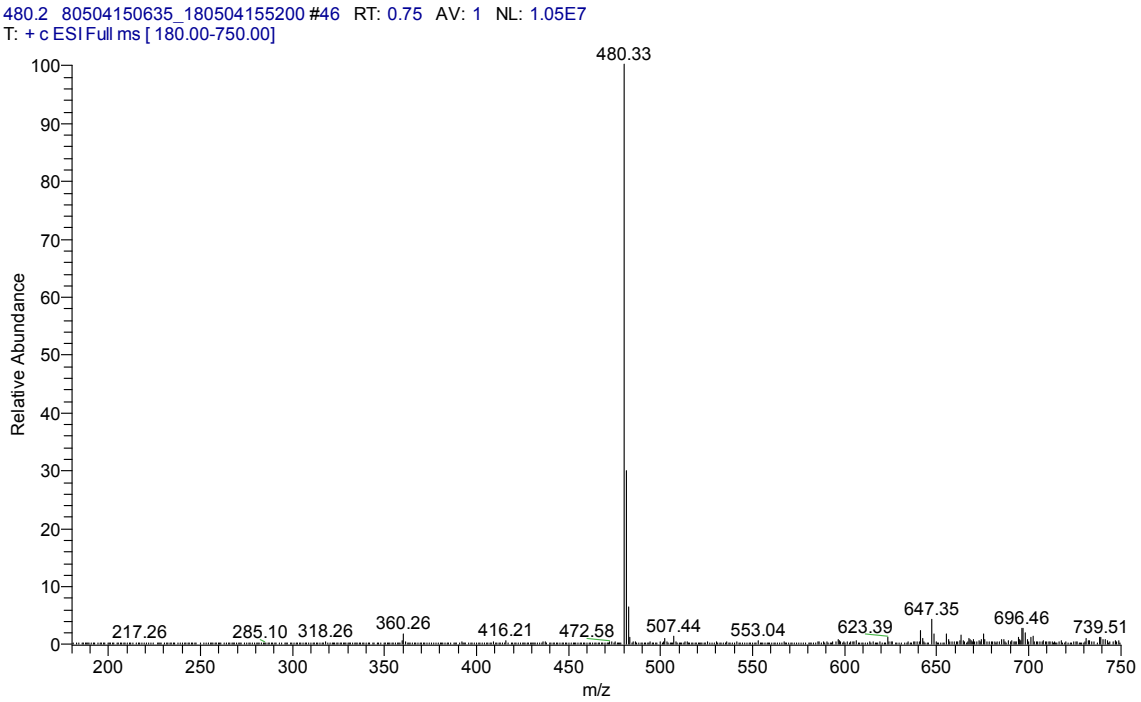

Fig. S25 ^{1}H NMR (400 MHz, DMSO-d_6) spectrum of Rhodol-NIR2.

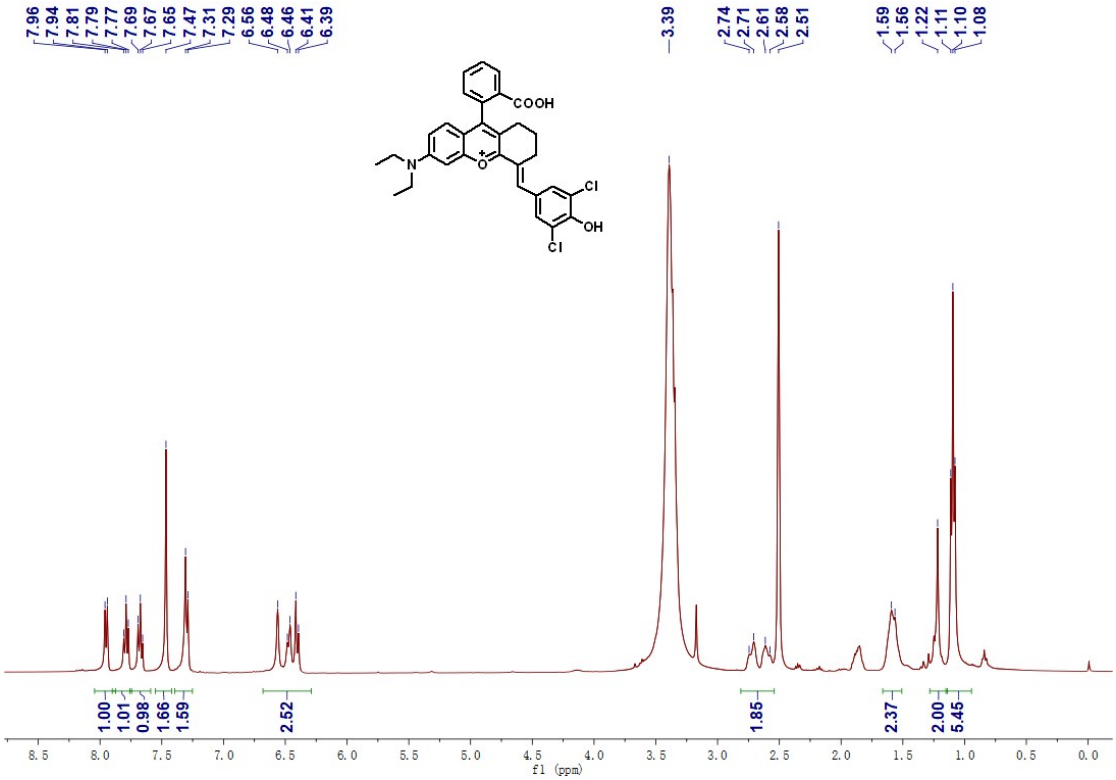

Fig. S26 ^{13}C NMR (100 MHz, DMSO-d_6) spectrum of Rhodol-NIR2.

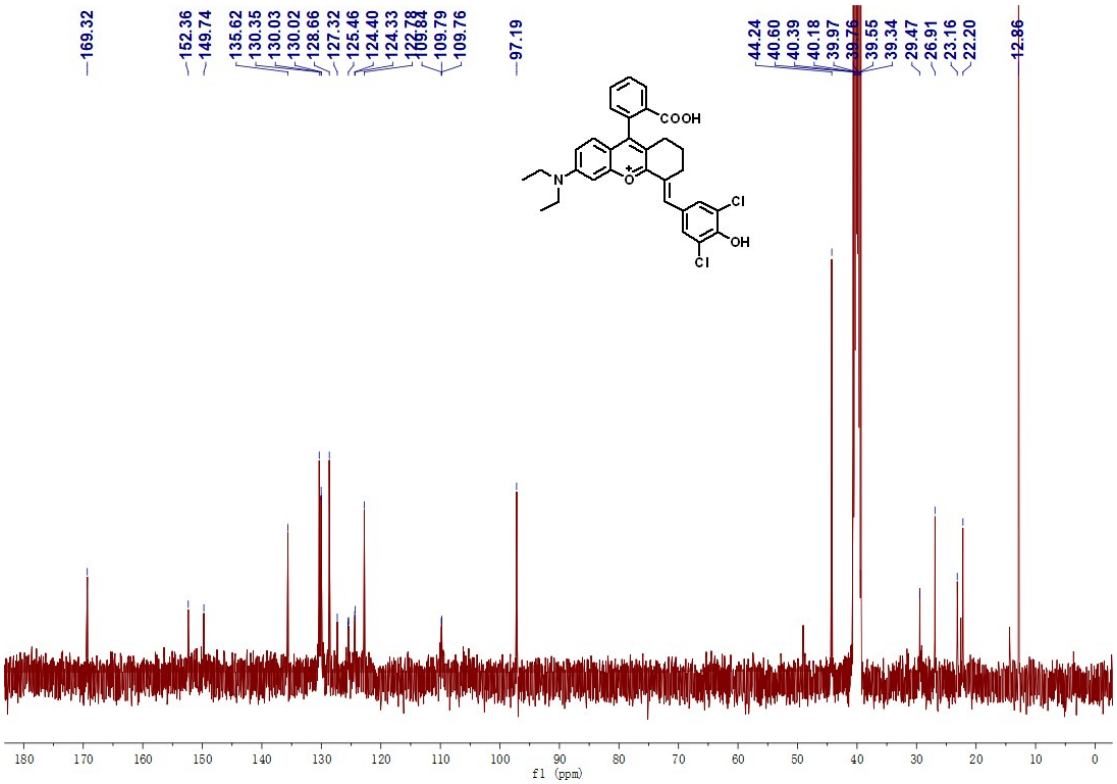

Fig. S27 ESI-MS spectrum of Rhodol-NIR2.

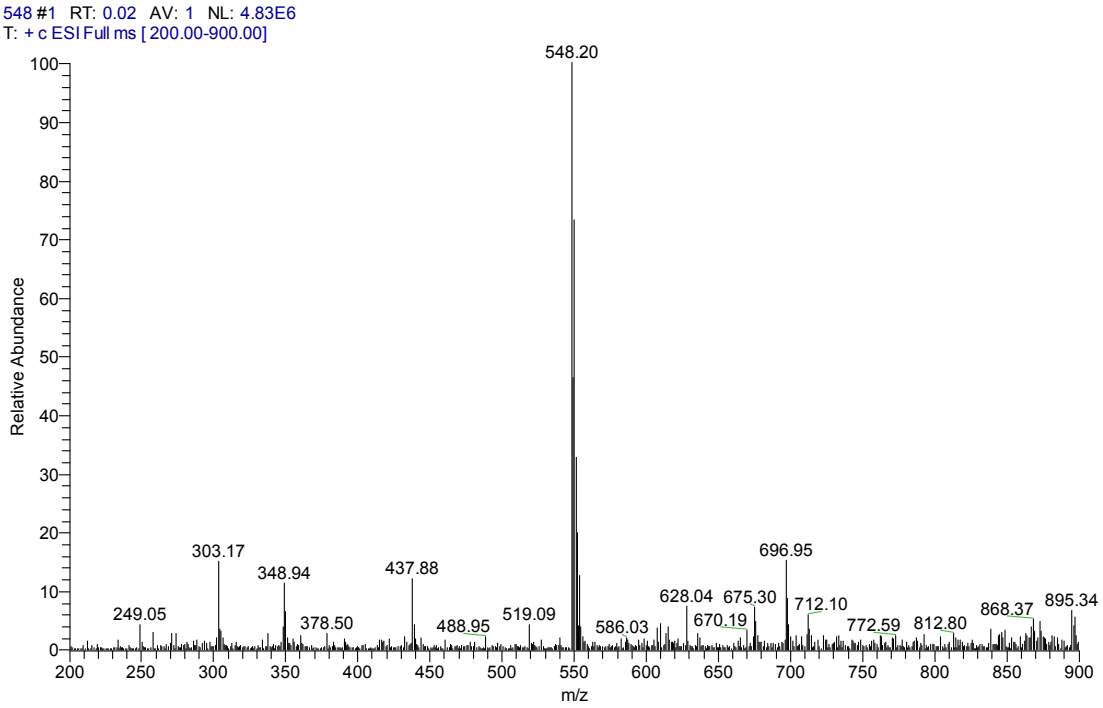

Fig. S28 ^{1}H NMR (400 MHz, DMSO-d_6) spectrum of Rhodol-NIR.

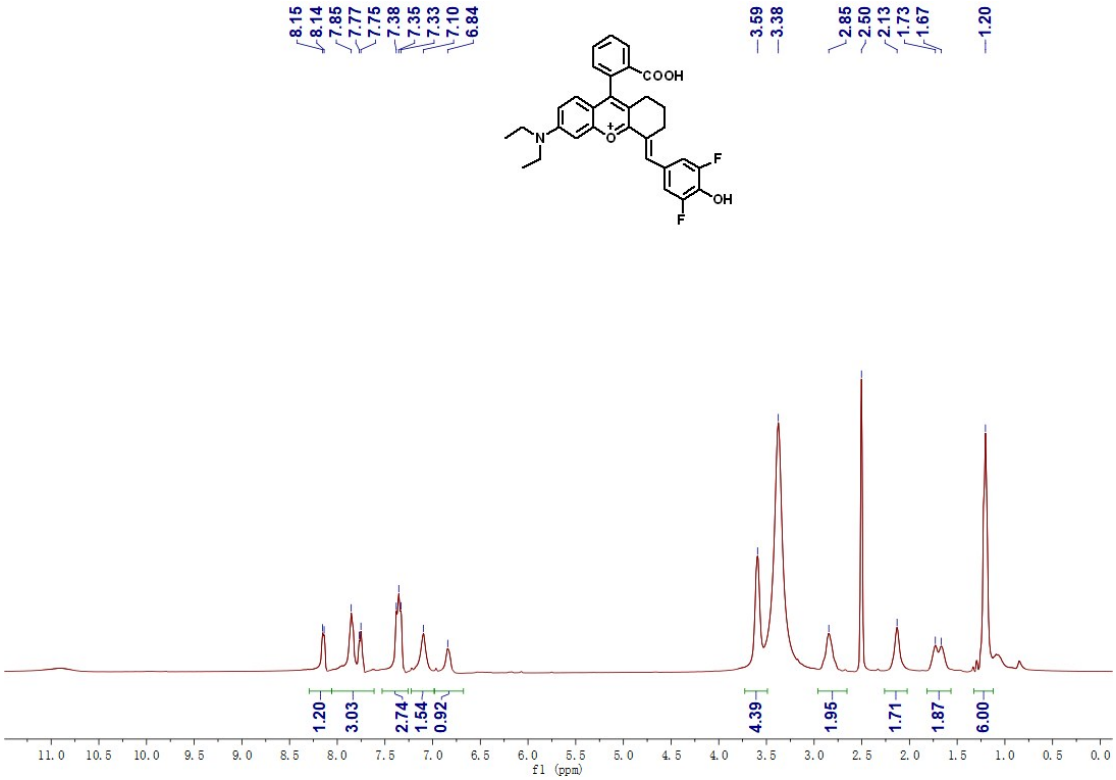

Fig. S29 ^{13}C NMR (100 MHz, DMSO-d_6) spectrum of Rhodol-NIR.

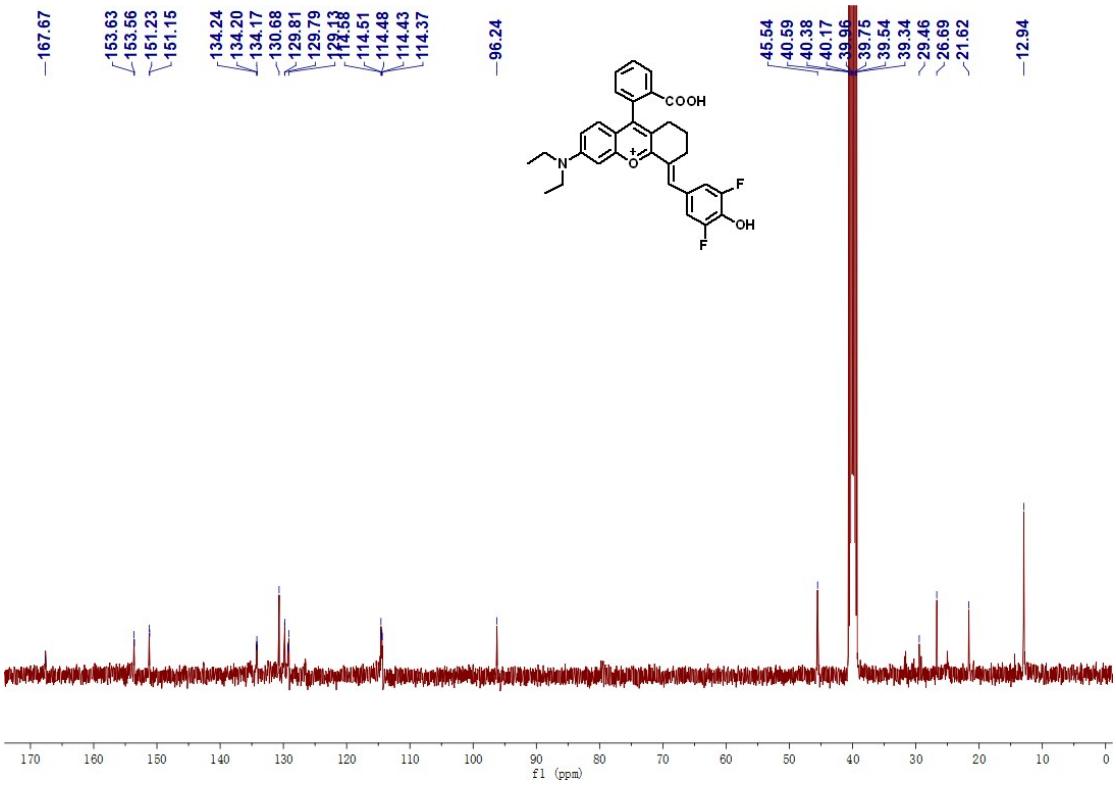

Fig. S30 ^{19}F NMR (400 MHz, DMSO-d_6) spectrum of Rhodol-NIR.

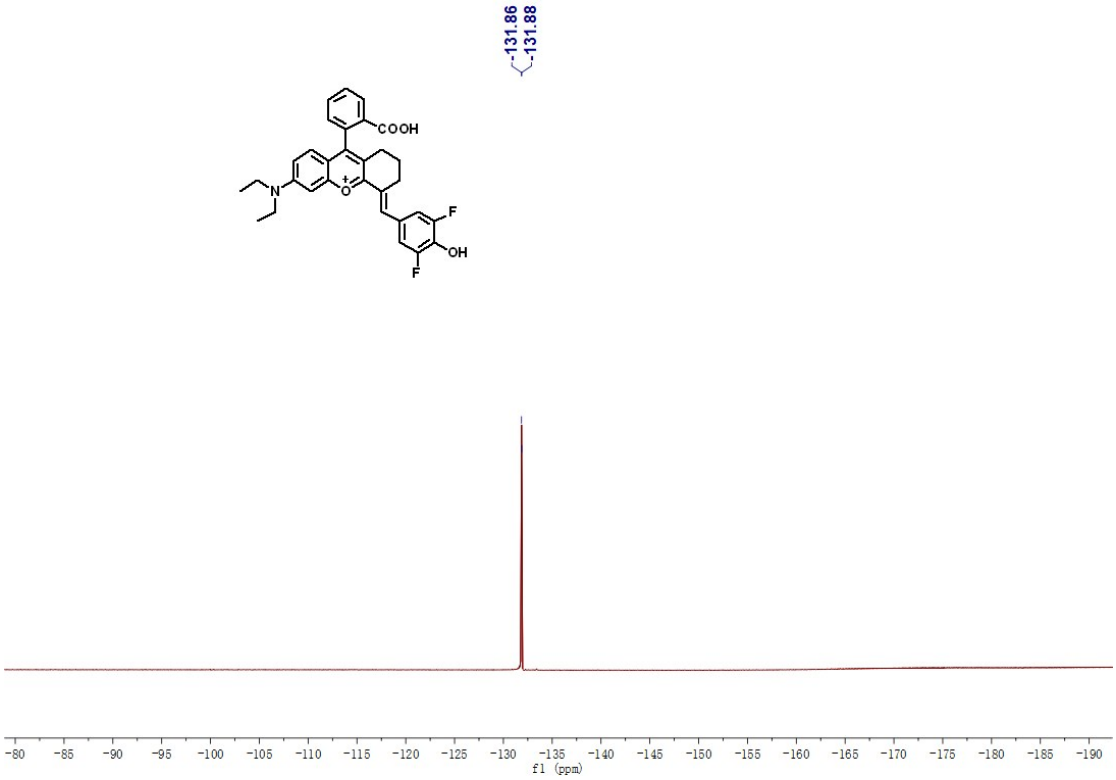

Fig. S31 HRMS (ESI) spectrum of Rhodol-NIR.

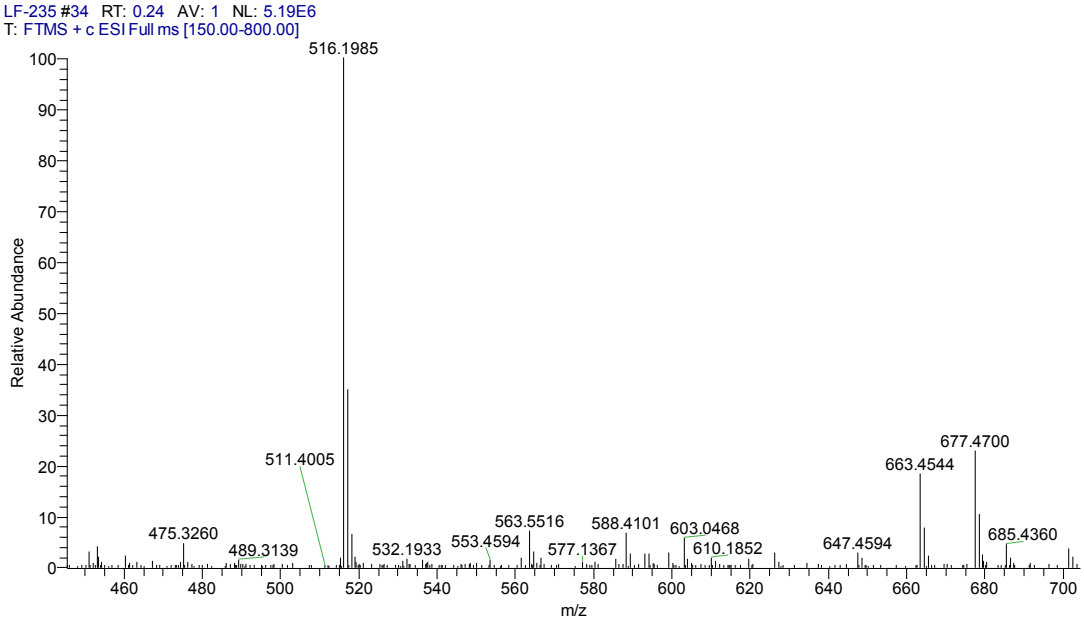

Fig. S32 ^{1}H NMR (400 MHz, DMSO-d_6) spectrum of Control chromophore.

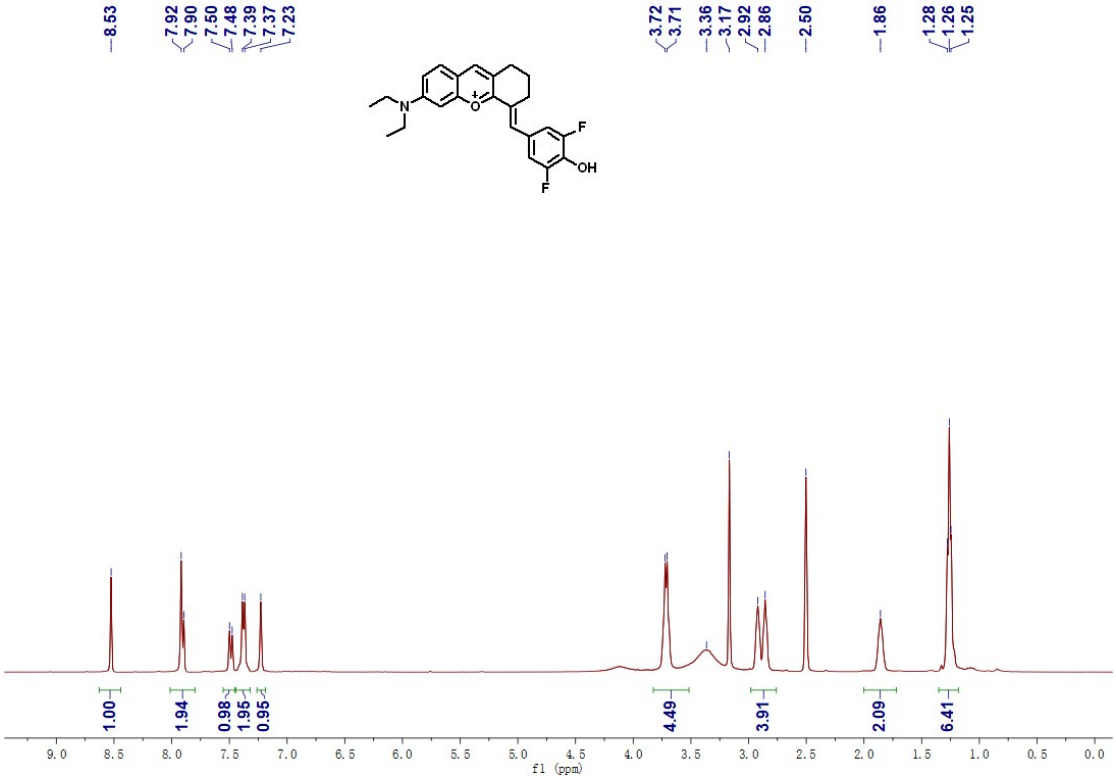

Fig. S33 ^{13}C NMR (100 MHz, DMSO-d_6) spectrum of Control chromophore.

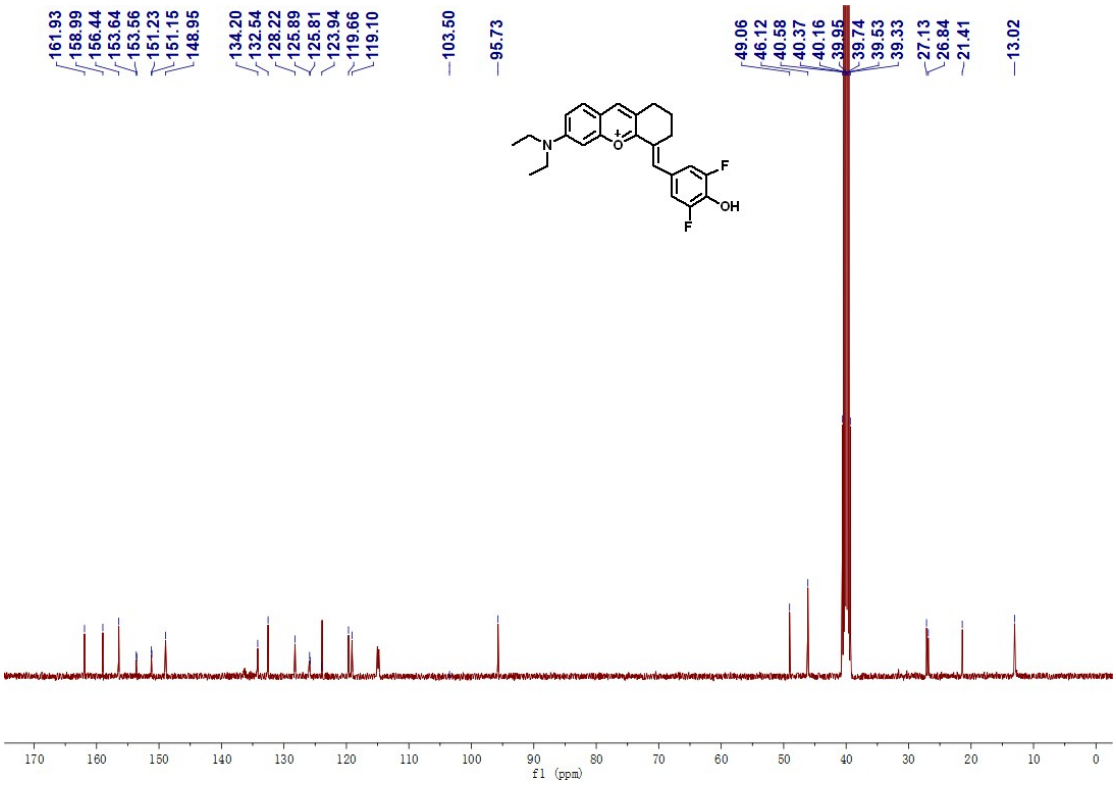

Fig. S34 ^{19}F NMR (400 MHz, DMSO-d_6) spectrum of Control chromophore.

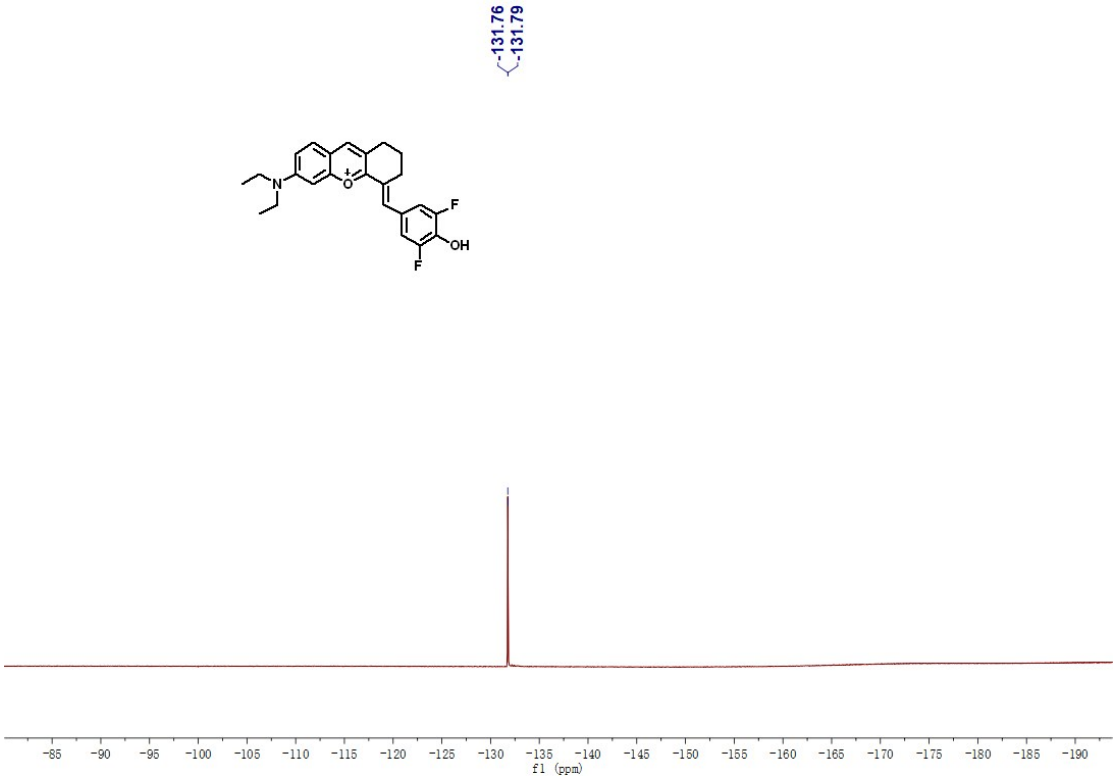

Fig. S35 ESI-MS spectrum of Control chromophore.

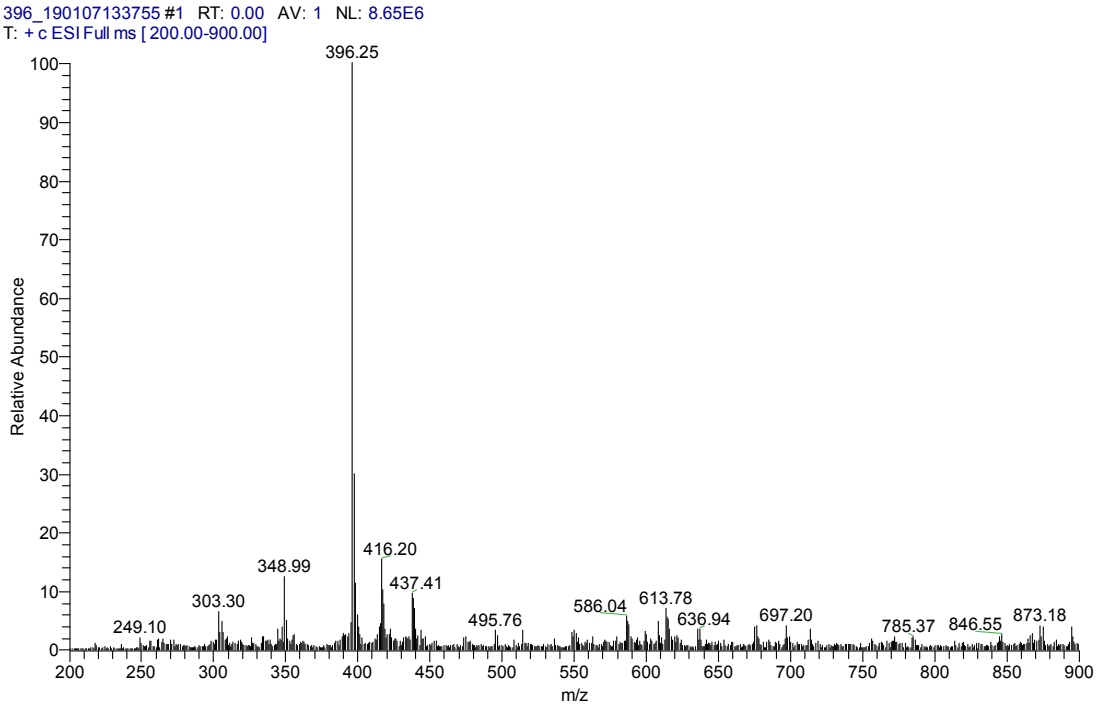

Fig. S36 ^{1}H NMR (400 MHz, DMSO-d_6) spectrum of acetylated Rhodol-NIR.

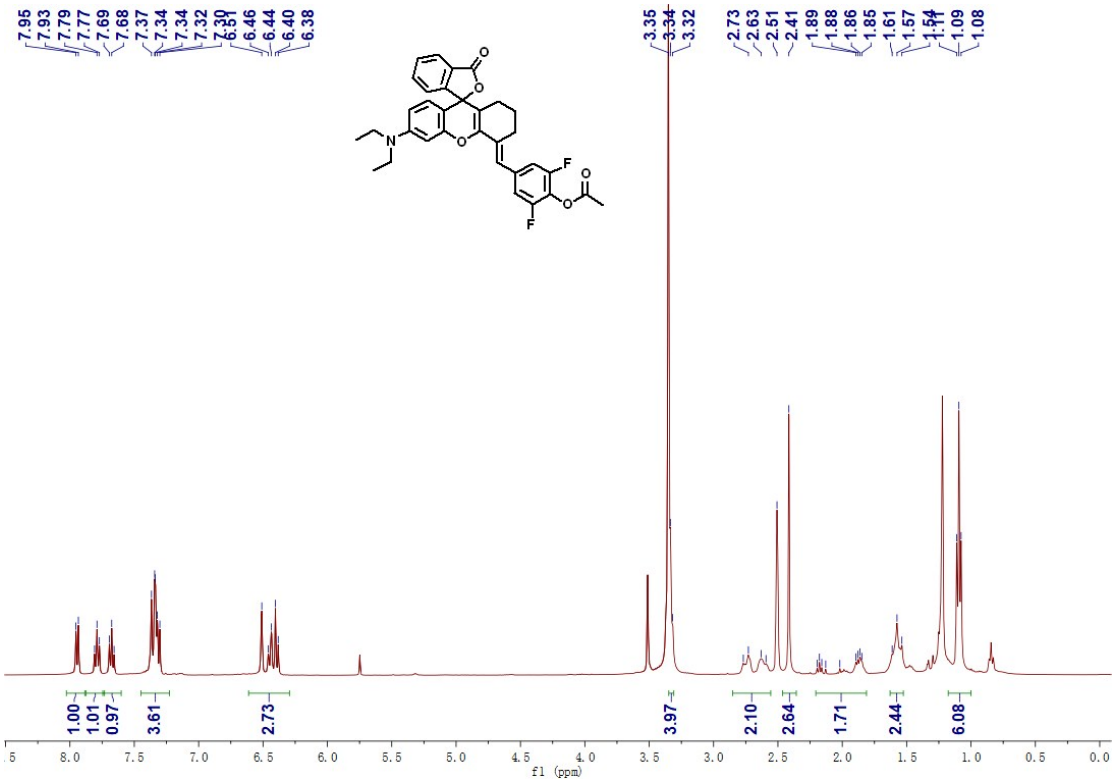

Fig. S37 ^{13}C NMR (100 MHz, DMSO-d_6) spectrum of acetylated Rhodol-NIR.

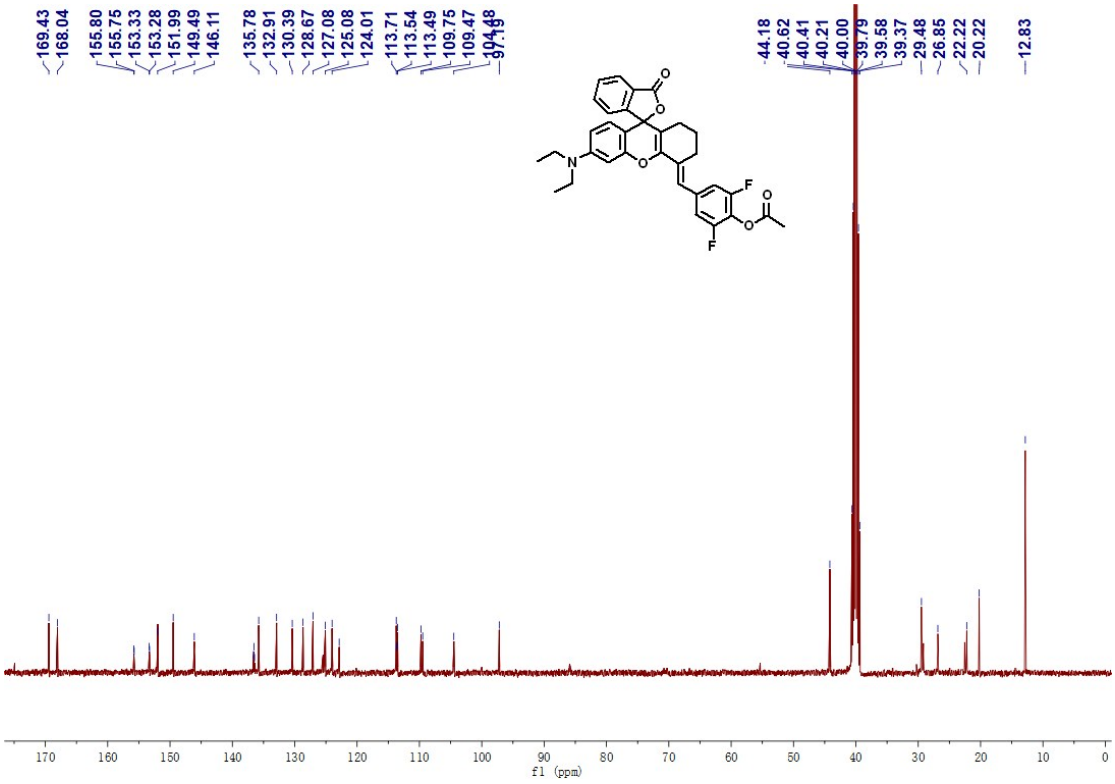

Fig. S38 ^{19}F NMR (400 MHz, DMSO-d_6) spectrum of acetylated Rhodol-NIR.

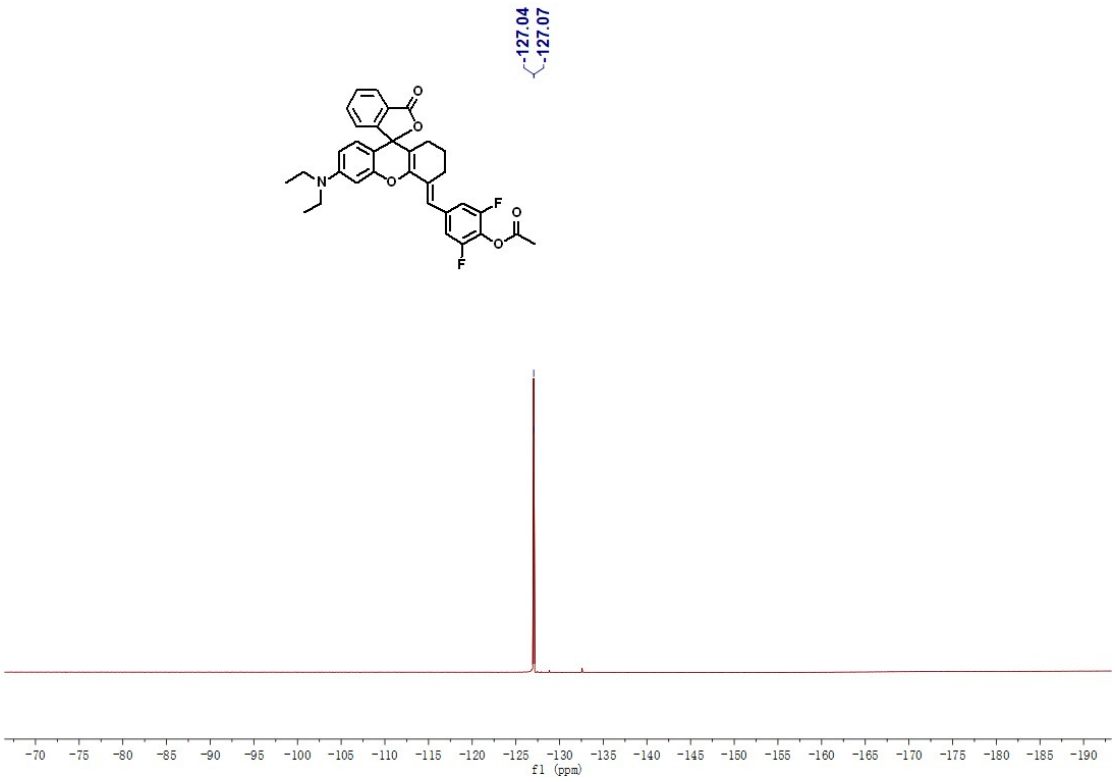

Fig. S39 ESI-MS spectrum of acetylated Rhodol-NIR.

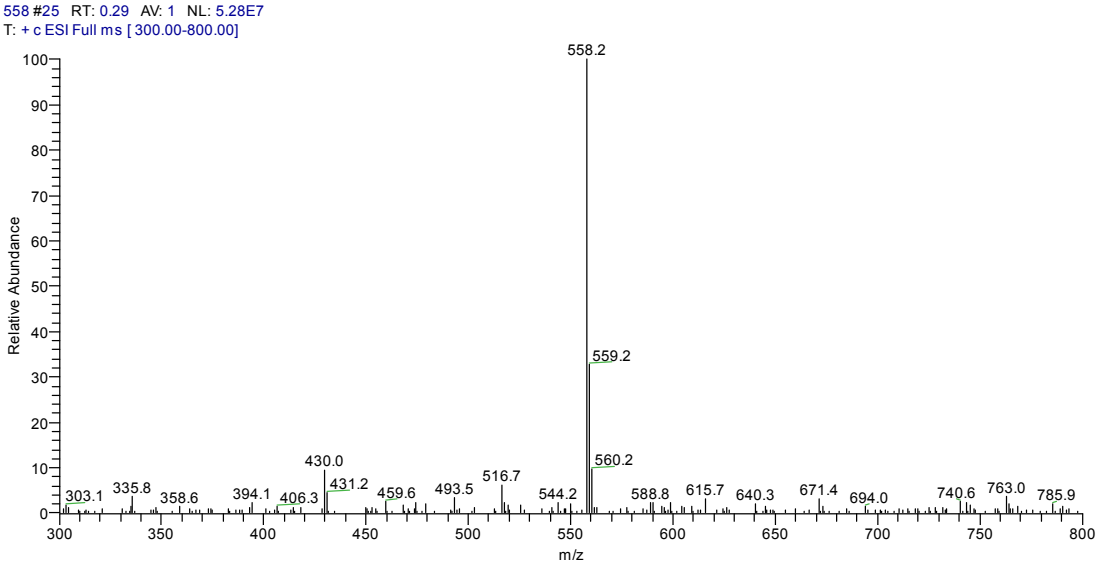

Fig. S40 ESI-MS spectrum of Rhodol-NIR3.

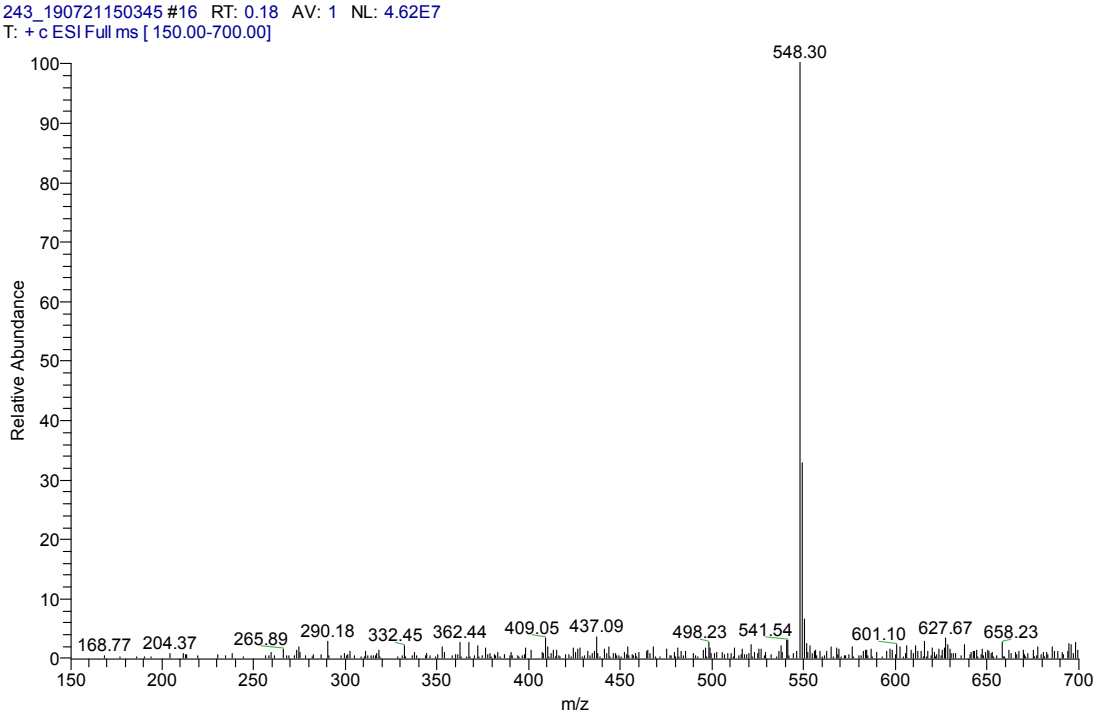

Fig. S41 ESI-MS spectrum of acetylated Rhodol-NIR3.

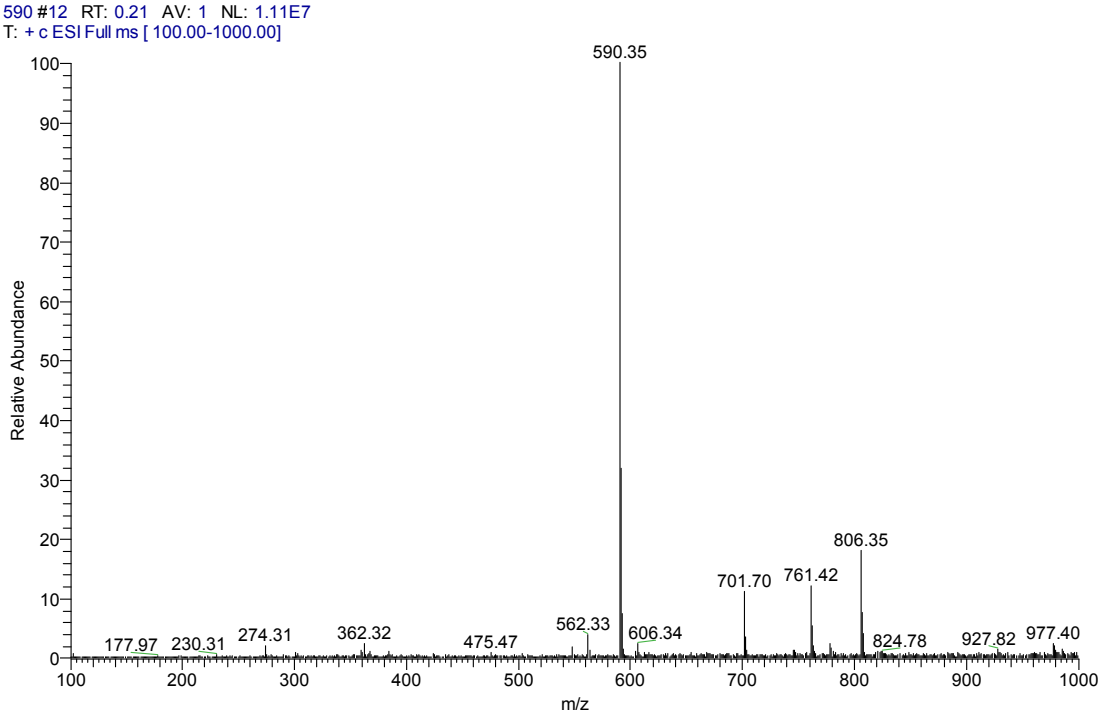

Fig. S42 ESI-MS spectrum of Rhodol-NIR4.

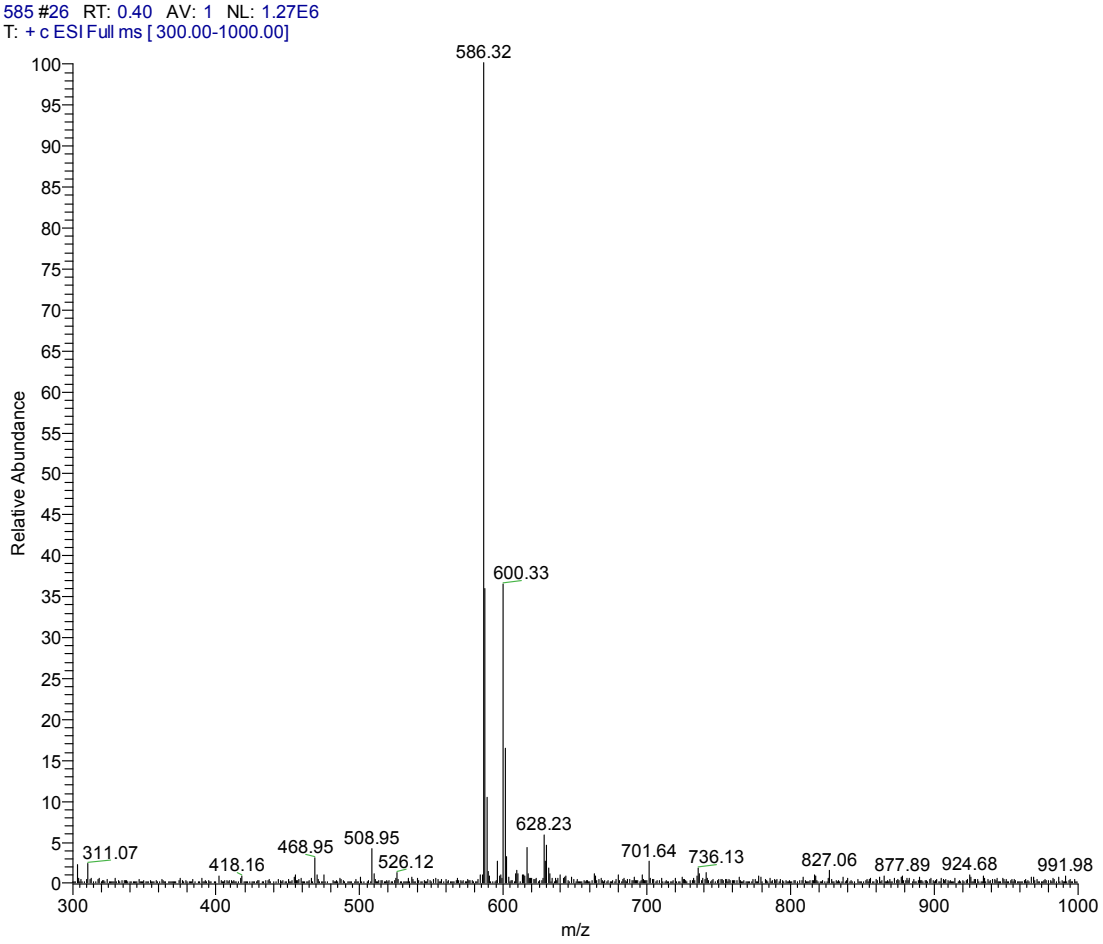

Fig. S43 ESI-MS spectrum of acetylated Rhodol-NIR4.

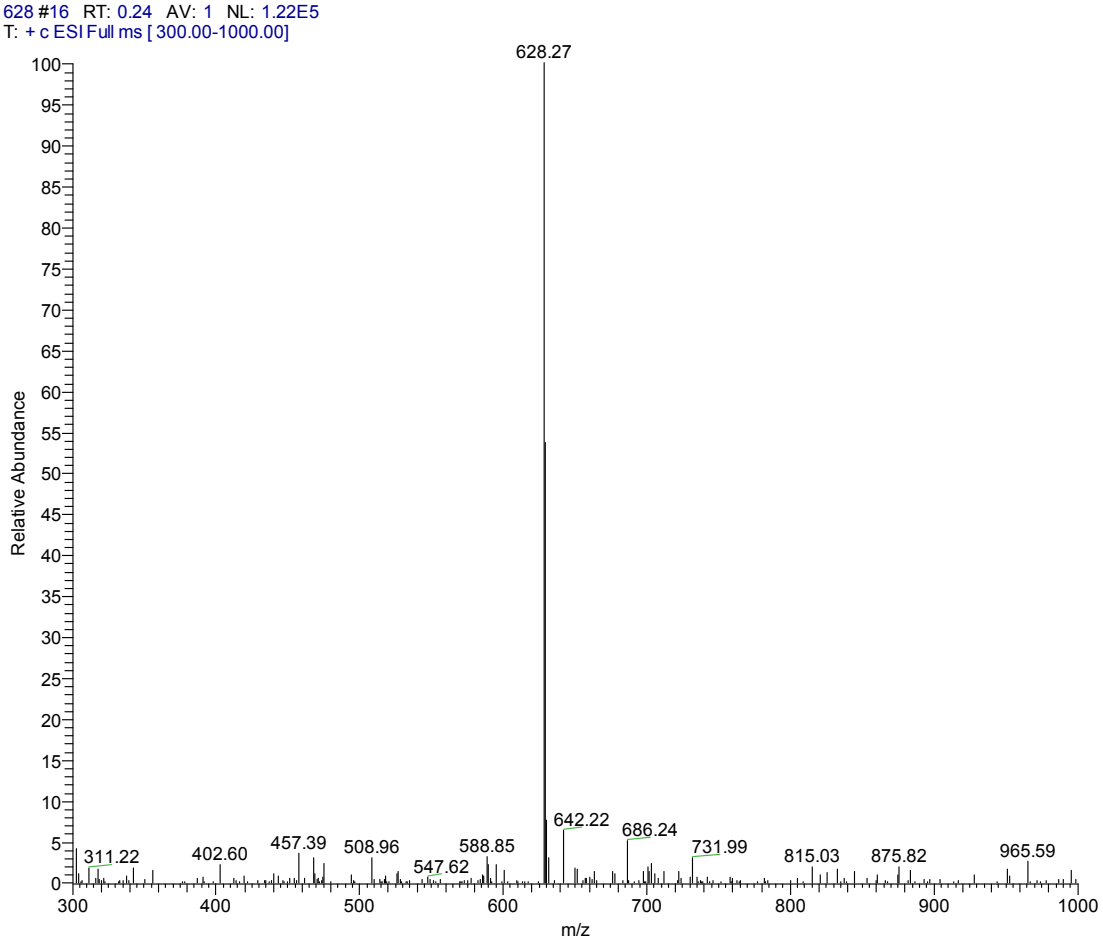

Fig. S44 ^{1}H NMR (400 MHz, CD_3Cl) spectrum of Rhodol-PA.

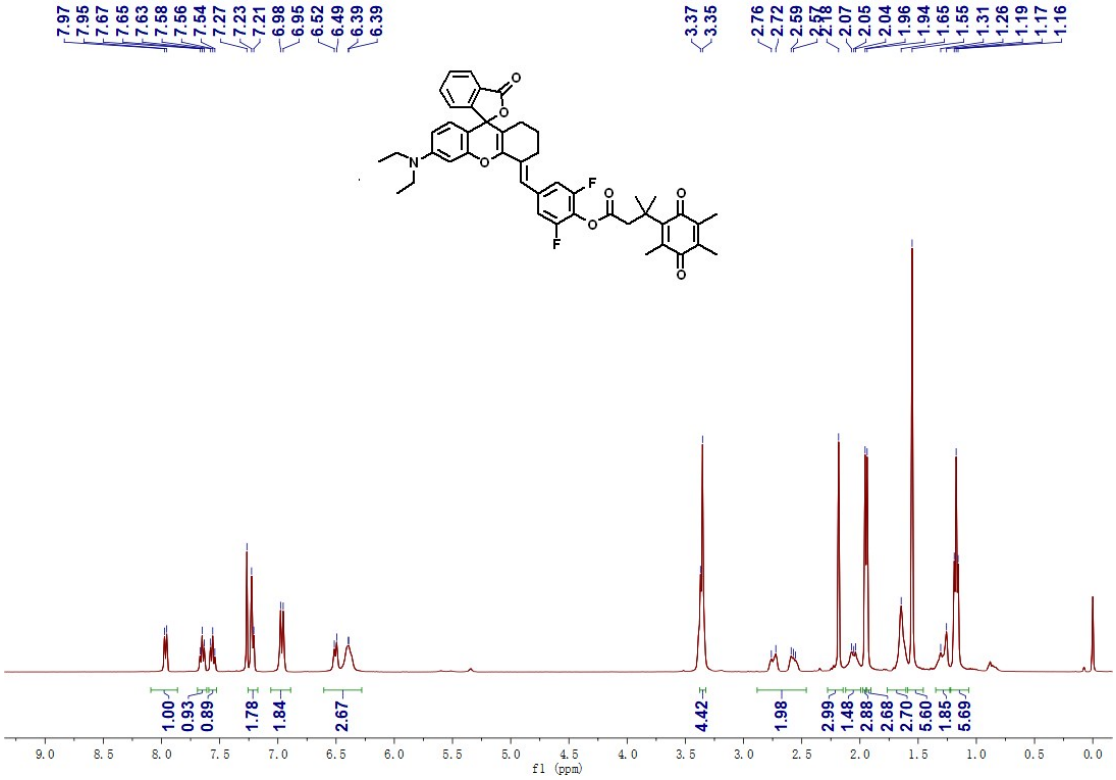

Fig. S45 ^{13}C NMR (100 MHz, CD_3Cl) spectrum of Rhodol-PA.

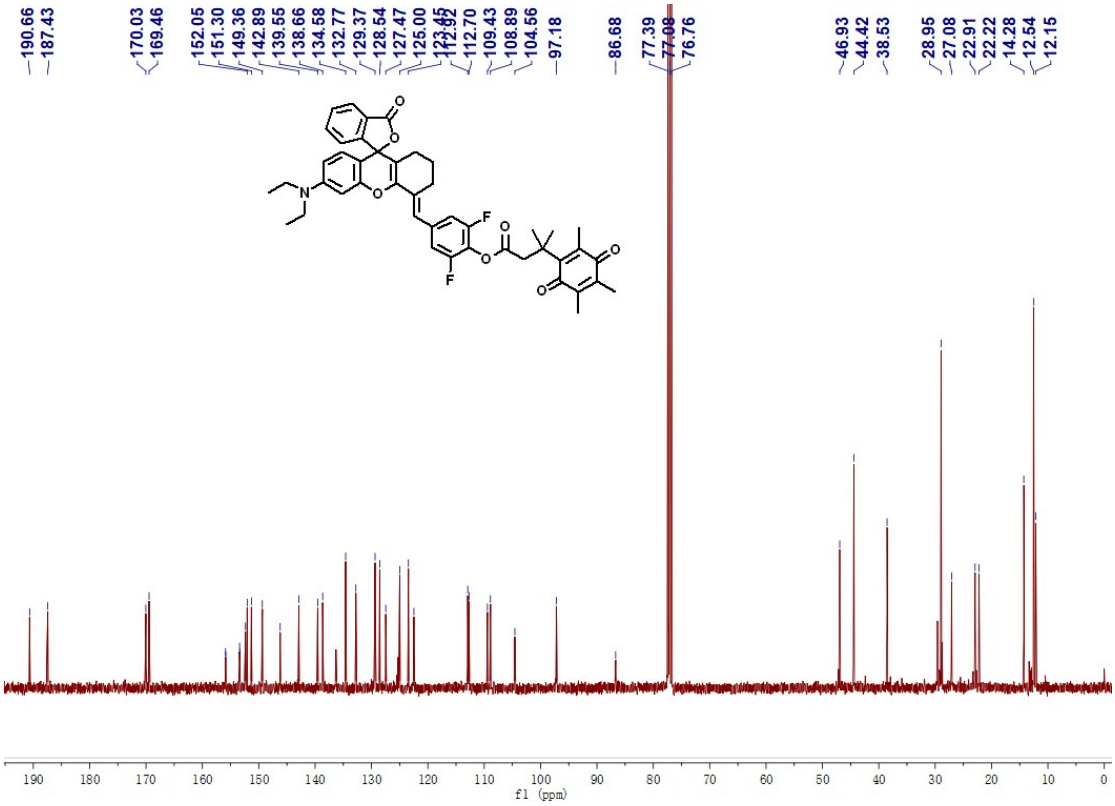

Fig. S46 ^{19}F NMR (400 MHz, DMSO-d_6) spectrum of Rhodol-PA.

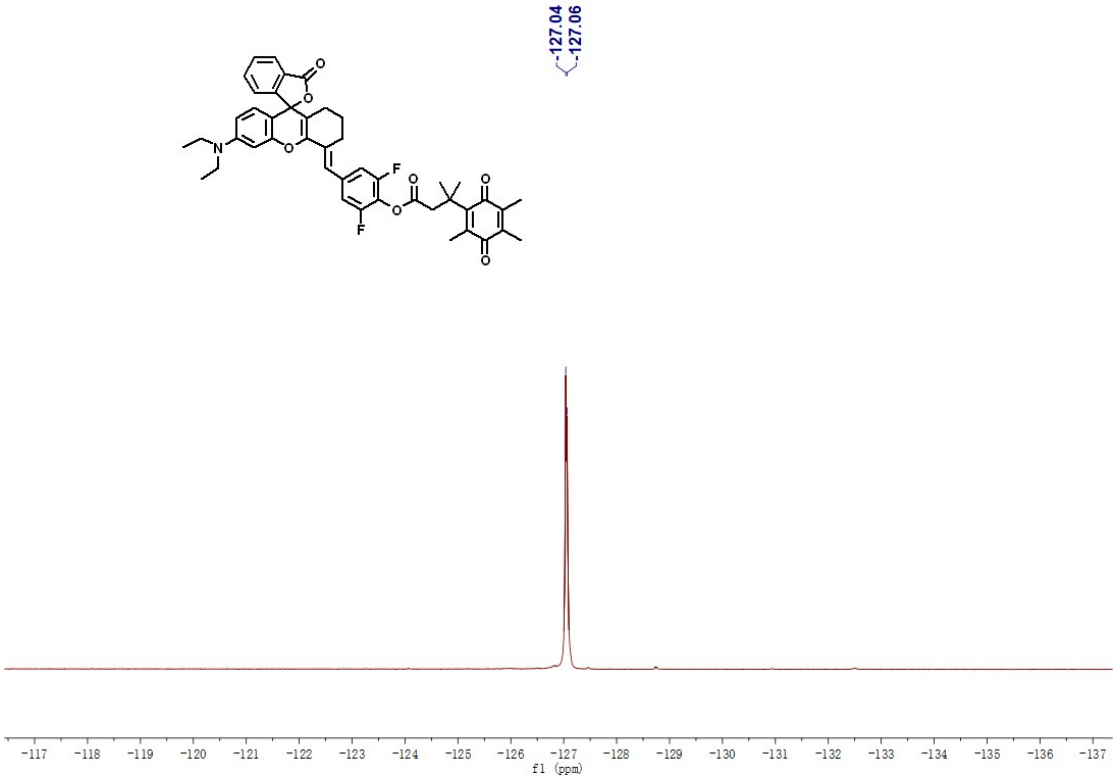

Fig. S47 HRMS (ESI) spectrum of Rhodol-PA.

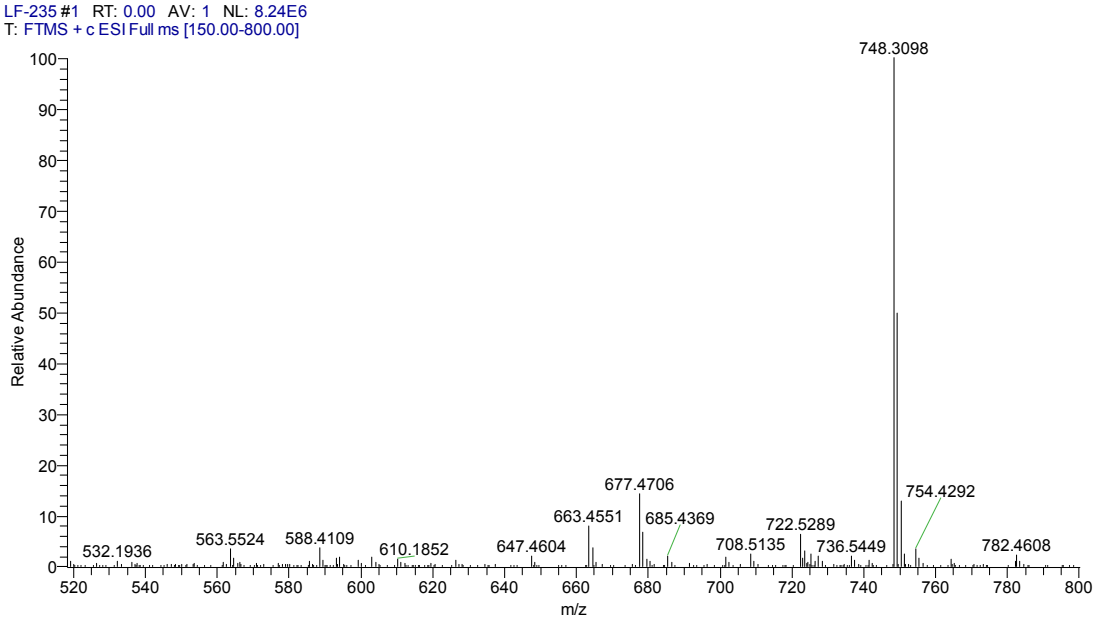

Fig. S48 ^{1}H NMR (400 MHz, CD_3Cl) spectrum of Control probe.

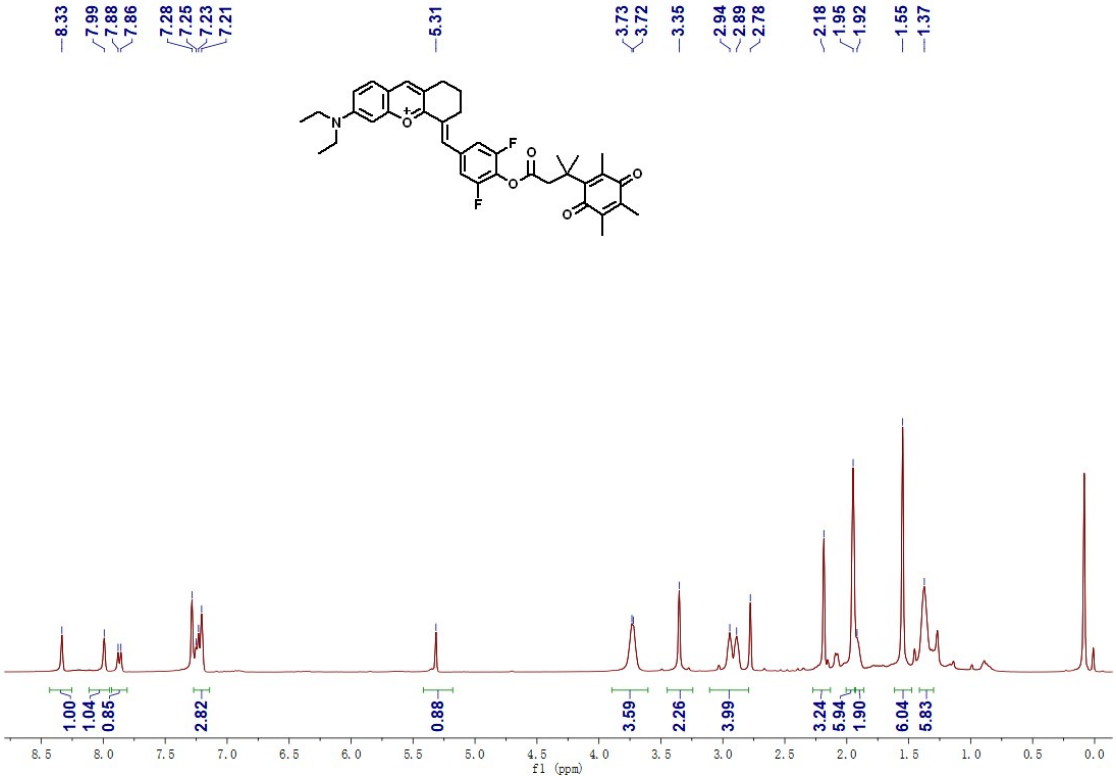

Fig. S49 ^{13}C NMR (100 MHz, CD_3Cl) spectrum of Control probe.

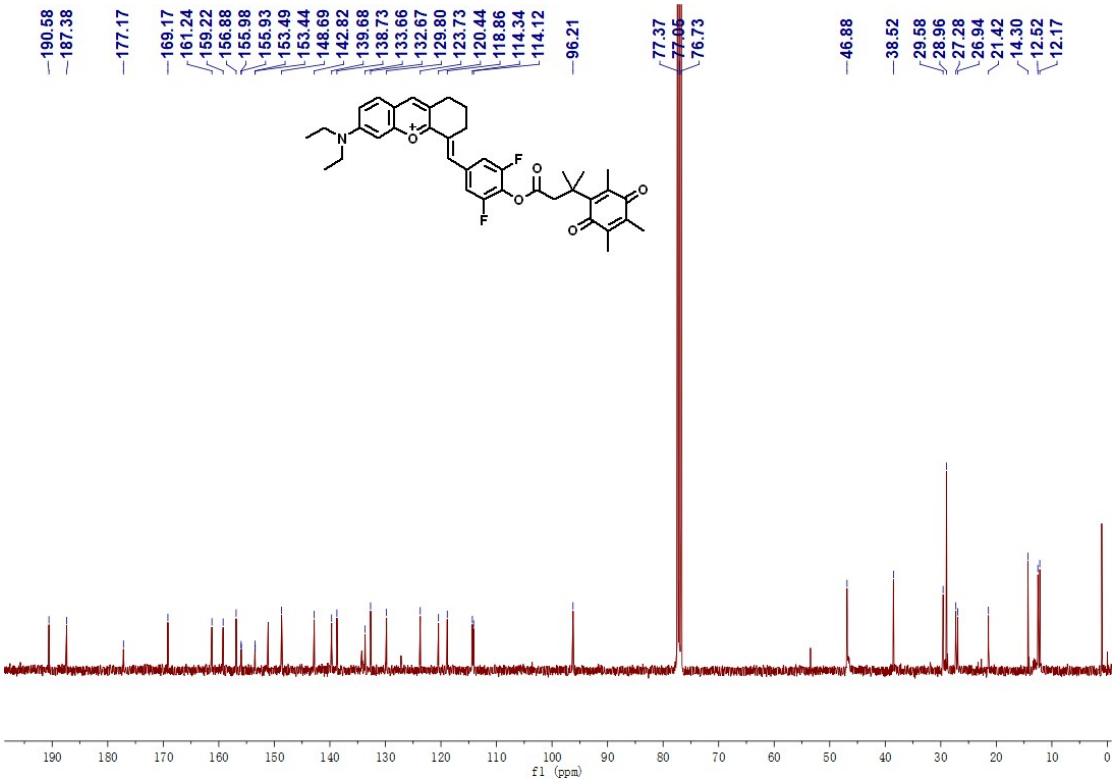

Fig. S50 ^{19}F NMR (400 MHz, CD_3Cl) spectrum of Control probe.

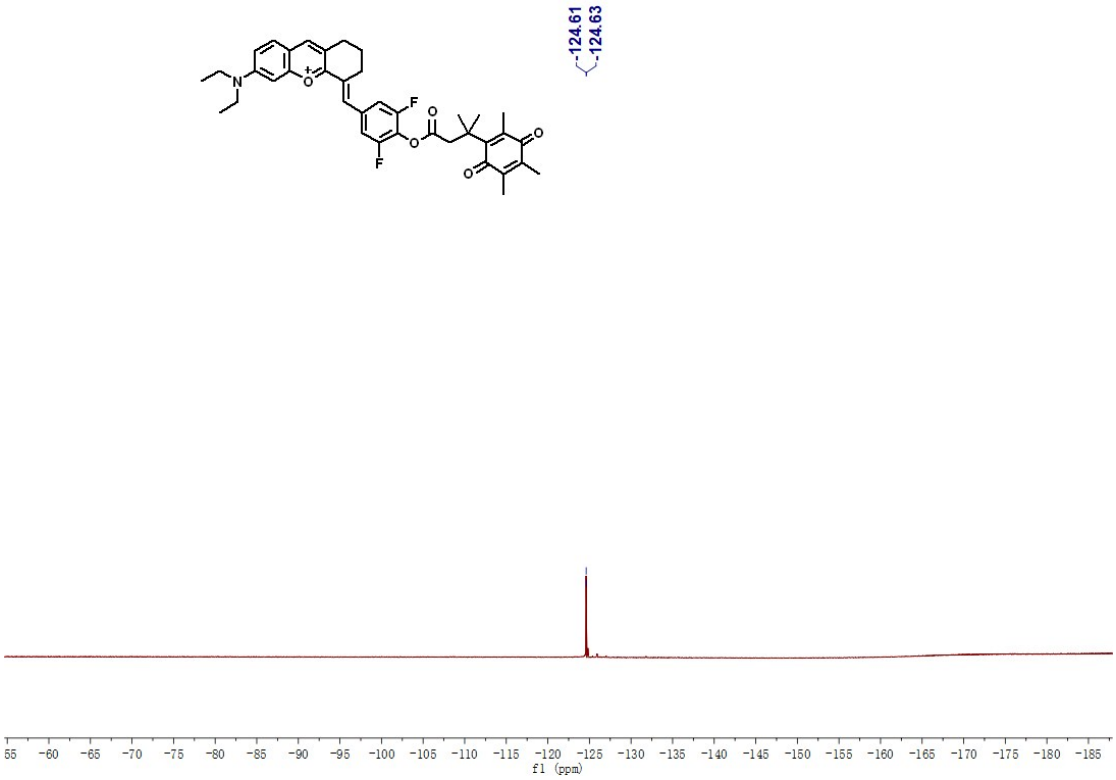

Fig. S51 HRMS (ESI) spectrum of Control probe.